Glasses: Aluminosilicates

Laurent Cormier

Glasses: Aluminosilicates

Laurent Cormier

Sorbonne Université, Muséum National d'Histoire Naturelle, UMR CNRS 7590, Institut de Minéralogie, de Physique des Matériaux et de Cosmochimie, IMPMC, 75005 Paris, France

Email : laurent.cormier@sorbonne-universite.fr

Keywords : aluminosilicate; aluminate; glasses; structure; rare-earth; viscosity; mechanical properties; coordination; NMR; diffraction

---

Abstract

Aluminosilicate glasses are of great importance for industrial applications and are good analogues of magmas. In practical applications, almost all silicate glasses incorporate alumina either as impurity or as a large component and Al_2O_3 usually imparts greater chemical durability, viscosity, glass transformation temperatures, improves mechanical properties, reduces devitrification tendencies and thermal expansion. Recent experimental and modelling techniques have substantially improved our understanding of the atomic-scale structure, providing a strong basis to better control glass properties. In this chapter, the composition-structure-property relationships in a great variety of glasses containing Al_2O_3 are reviewed.

Aluminosilicate glasses are widely used and investigated materials with current and promising technological applications such as high-power laser gain media, flat-panel displays, solid oxide fuel cells, sealing materials, glass-fiber composites and long-term immobilization of wastes, to name a few. They are also abundant in nature and relevant for geological processes as they are chemically close to the natural magmatic compositions of the Earth mantle. Finally at low SiO_2 content, quenched metallurgical slags are mainly composed of aluminosilicate glasses. Introducing Al_2O_3 strongly affects many physico-chemical properties. For instance, it improves fracture strength, increases elastic modulus and chemical resistance or hinders the trend to phase separation. Many properties correlate with the nature of non-framework cations present in the glass and to the flexibility for Al to adopt multiple coordination states. Different aspects of the disorder (network connectivity, Si/Al disorder, short range environment) affect the topological and configurational entropies. In this chapter we address the specificities of the atomic-scale structure in diverse glass models containing alumina with important implications for interpreting and controlling the physico-chemical properties.

Commercial Glasses

Aluminosilicate (AS) glasses, notably at low-alkali content, have high values of tensile strength, resistance to high temperature and excellence resistance to chemical corrosion (Varshneya and Mauro, 2019). They have found widespread commercial application as fibers to reinforce plastics or concrete. E-glass (a low-alkali Ca-Mg alumino-borosilicate glass with 10-15 mol.% Al_2O_3) is the most common glass fibers. Nowadays, a major application concerns alkali-free aluminosilicates used as thin glass sheets for liquid crystal flat displays.

With higher amounts of alkalis, aluminosilicate glasses can be used to obtain high surface strength via an ion exchange process. The chemical exchange (typically Na replaced by K) produces a permanent compressive stress in the glass surface that improves resistance to cracks and scratches. This type of glass is exploited in smartphone screens or aircraft windshields and further applications (for instance in automotive) are foreseen. Alkali or alkaline-earth aluminosilicate systems are also the precursor glasses for most glass-ceramics successfully designed for consumer applications.

Al_2O_3, the archetypical intermediate oxide

Al_2O_3 itself cannot form a glass as it does not satisfy the rules proposed by Zachariasen (1932) for a network former. However, a specificity of Al_2O_3 is to be able to form a glass when it is mixed

with some modifying cations (typically alkaline earths or rare-earths). Sun (1947) has classified Al_2O_3 as an intermediate oxide acting as network former or modifier according to the composition. Indeed, Al_2O_3 can be added into the vitreous silicate network by replacing Si^{4+} cations in a tetrahedral environment. In that case, it plays the role of a network former and even small amounts of Al_2O_3 considerably modify the glass properties. Alternatively, Al can enter into high coordinated sites, playing the role of a modifier

Basic structural features

Al in substitution for Si

Si is a network former occurring as SiO_4 tetrahedra in oxide glasses. In aluminosilicate glasses, Al has a strong preference for tetrahedral coordination and usually substitutes for Si in tetrahedral positions, behaving similarly to a network former. An $Al^{3+}O_4$ tetrahedron has a charge deficit compared to a $Si^{4+}O_4$ unit because only three positive charges are brought by Al^{3+} cations. The electrical balance and the stabilization of $(AlO_4)^-$ tetrahedra are ensured by introducing positive charges brought by alkali (M^+), alkaline earth (M^{2+}) or rare-earth (RE^{3+}) cations. The cations compensating the net negative charge on $(AlO_4)^-$ units are called charge compensators (or charge-balancing cations), as opposed to a network modifying role when they are associated with non-bridging oxygen atoms (NBOs), participating in this latter case to the loss of network connectivity (depolymerization). A schematic representation of the addition of Al_2O_3 in a silicate glass network is shown in figure 1. The introduction of Al_2O_3 results in less NBOs (and thus more bridging oxygen atoms, BOs) and increases network connectivity. As a consequence the network becomes more stiff, the viscosity and the glass transition temperature (T_g) increase.

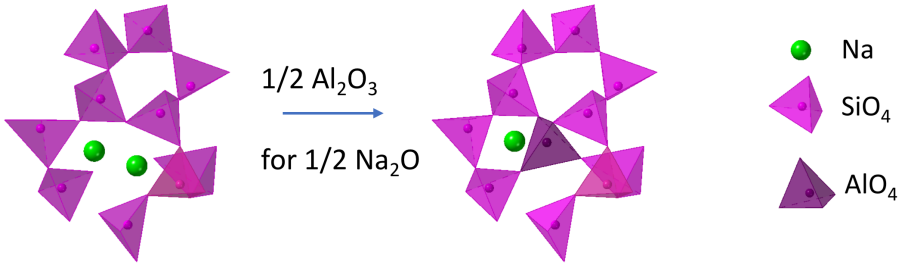

Figure 1. Schematic representation of replacement of ½Na_2O by ½Al_2O_3, resulting in a pair of non-bridging oxygens replaced by one bridging oxygen.

Since the Al-O bond length (1.76 Å) is longer than for Si-O (1.62 Å) (Cormier et al., 2000b), the AlO_4 tetrahedron is bigger than SiO_4. The replacement of Si by Al then modifies the network organization and changes the glass physico-chemical properties. Raman spectroscopic investigations of aluminosilicate glasses (Mysen, 1990) revealed that increasing the Al/Si ratio implies a decrease in the force constant due to the weakening of the T-O bonds (T = Si or Al) when Al substitutes for Si. The structure of aluminosilicate glasses largely depends on the arrangement of SiO_4 and AlO_4 tetrahedra that are forming a skeletal network by corner-sharing through bridging oxygen (BO) atoms.

The network connectivity is efficiently probed by Magic-angle spinning (MAS) nuclear magnetic resonance (NMR) spectroscopy. The NMR chemical shift of ^{29}Si is sensitive to the degree of connectivity of the SiO_4 tetrahedra represented by the Q^n notation with n the number of BO on a tetrahedron. The decreasing number of BO displaces the chemical shift to higher values. The Si/Al substitution causes an additional modification of the chemical shift depending on the number m of Al atoms as second neighbors (figure 2). The moieties for Si and Al are denoted $Q_{Si}^n(mAl)$ and $Q_{Al}^n(mSi)$, respectively, indicating m Si-O-Al or Al-O-Si bonds (Edén, 2015). A Q_{Al}^3 unit with a negative charge (-2) and one NBO requires a greater number of charge balancing cations in its neighborhood compared to a Q_{Si}^3 with a charge (-1). The fully connected Q_{Al}^4 species (charge -1) are then favored. Though the different $Q_{Si}^n(mAl)$ moieties strongly overlap in the ^{29}Si NMR signal, advanced NMR techniques allow the relative amounts of these species to be fully quantified (Hiet, 2009).

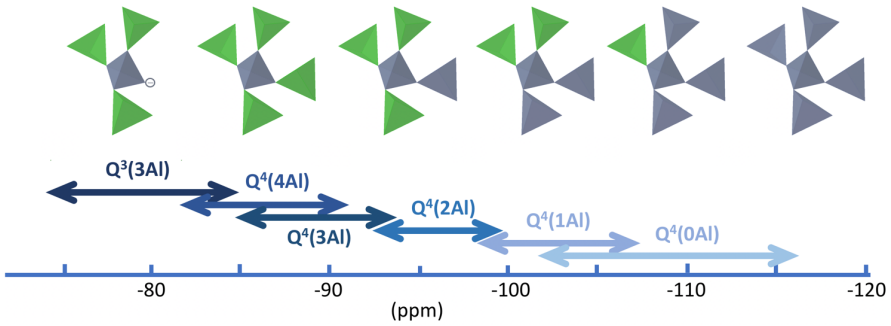

Figure 2. Changes of the ^{29}Si chemical shifts for the various $Q_{Si}^n(mAl)$ units in aluminosilicate glasses, as proposed by (Engelhardt, 1989).

Another important structural feature is to determine the extent of Si/Al ordering that can be revealed by ^{17}O NMR. This spectroscopy gives access to the various linkages between BO atoms and framework cations, i.e. $^{[4]}$Si-O-$^{[4]}$Si, $^{[4]}$Si-O-$^{[4,5]}$Al, and $^{[4]}$Al-O-$^{[4,5]}$Al. Extensive Si/Al mixing,

reflecting chemical order, results in a high fraction of $^{[4]}$Si-O-$^{[4]}$Al, whereas a tendency toward disorder leads to high fractions of $^{[4]}$Al-O-$^{[4]}$Al and $^{[4]}$Si-O-$^{[4]}$Si (Lee and Stebbins, 2002).

Al avoidance principle

According to the Loewenstein's rule (Loewenstein, 1954), also known as the Al-avoidance principle, there is a strong preference for $^{[4]}$Si-O-$^{[4]}$Al linkages, whereas those of $^{[4]}$Al-O-$^{[4]}$Al are energetically less favorable and avoided due to the local negative charge-accumulation. This rule governs the distribution of framework cations within the network but it seems to suffer many exceptions in alkali/alkaline-earth/rare-earth aluminosilicate glasses (Lee and Stebbins, 1999; S.K. Lee and Stebbins, 2000a; Lee et al., 2005; Moesgaard et al., 2010; Jaworski et al., 2015). The framework disorder is quantified by the $Q_{Si}^{n}(mAl)$ moieties or the oxygen cluster population, T-O-T, that both can be ascertained experimentally using MAS-NMR spectroscopy of ^{29}Si and ^{17}O nuclei and confirmed with many molecular dynamics (MD) simulations (Lee and Stebbins, 1999; S.K. Lee and Stebbins, 2000a; Lee and Stebbins, 2002; Lee et al., 2005; Lee and Stebbins, 2006; Moesgaard et al., 2010; Park and Lee, 2012; Jaworski et al., 2015).

To quantify the abundance of Si/Al intermixing, the degree of Al avoidance (Q) was proposed, spanning from complete chemical order (Q = 1, complete Al avoidance) to a random distribution of Si and Al (Q = 0) (Lee and Stebbins, 1999; Lee and Stebbins, 2002). At low Al_2O_3 content, obedience to the Loewenstein's rule is generally valid and implies a non-random mixing of network forming cations (Ando et al., 2018; Ganisetti et al., 2019). However, the proportion of Al-O-Al and Si-O-Al linkages increases with increasing connectivity as more Al_2O_3 is introduced at constant silica content (Lee and Stebbins, 2006; Lee and Stebbins, 2009). For instance, chemical ordering (Q = 0) is prevalent in Na aluminosilicate compositions except for compositions with $Na_2O/Al_2O_3 = 1$, emphasizing that the Si/Al ordering behavior depends on composition (Na/Si or Si/Al ratios) (Lee and Stebbins, 2000b; Lee et al., 2005; Iftekhar et al., 2009; Lee and Stebbins, 2009; Park and Lee, 2014). Increasing fictive temperatures tend to increase Al-O-Al linkages (Dubinsky, 2006). The size and valence of non-framework cations have also a considerable influence and this effect can be rationalized using the cation field strength, CFS, defined as z/r^2, with z the cation valence and r the ionic radius (Shannon, 1976). Since high CFS favors negative charge concentration, Al atoms tend to be closer and the probability of finding Al-O-Al linkages increases with CFS: RE > Mg > Ca < (Ba, Li) < Na < (K, Rb, Cs) (RE = rare earth) (Stebbins, 1999; Lee and Stebbins, 2000b; Lee and Stebbins, 2000a; Kelsey et al., 2008; Jaworski et al., 2012; Okhotnikov et al., 2013; Lee et al., 2016). Therefore, RE-aluminosilicate glasses display the highest degree of randomness in their Si/Al distribution (Iftekhar et al., 2009). Breakdown of the Al avoidance is confirmed by several MD simulations (Stein and Spera, 1995; Cormier et al., 2003; Ando et al., 2018; Ganisetti et al., 2019). The effect of CFS on

the degree of Al avoidance is shown in figure 3 for alkali/alkaline earth cations (Lee et al., 2016). The extent of chemical ordering (Q) manifests a linear decrease with CFS ($Q \approx -0.1 \times CFS + 1$). It is expected that this simple relationship could not be valid for glasses with higher CFS and/or with RE, with a deviation from the linear trend (Lee et al., 2016).

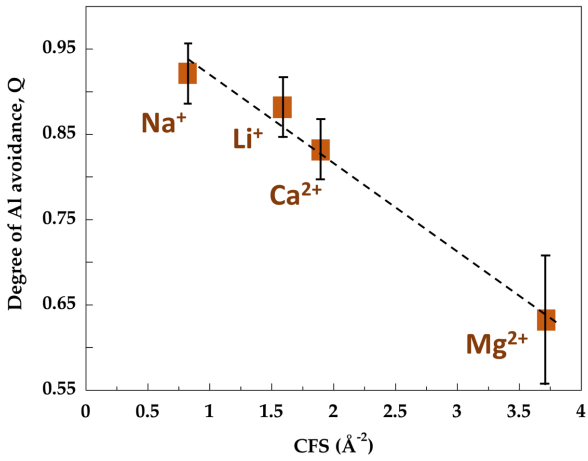

Figure 3. Effect of cation field strength, CFS, on the degree of Al avoidance, Q. Data from (Lee et al., 2016).

Aluminosilicate glass models

For tectosilicate compositions ($M^{n+}/n\mathrm{Al} = 1$), the fully interconnected network is described by the "Compensated Continuous Random Network" (CCRN) model (Greaves and Ngai, 1995a). The modified random network (MRN) model is used to describe Al_2O_3-free glasses and imply a micro-segregation of modifiers with the co-existence of two sub-networks: one rich in modifiers and NBOs and another one rich in network formers. For peralkaline(-earth) glasses ($M^{n+}/n\mathrm{Al} > 1$), an intermediate structure between CCRN and MRN prevails. Si^{4+} and Al^{3+} cations are essentially organized in a corner-sharing tetrahedral network with NBOs mainly connected to Si atoms. The M^{n+} cations not used to neutralize the charge-imbalance from $(AlO_4)^-$ tetrahedra promote the formation of NBOs. Percolating channels similar to those existing in the MRN models have also been proposed in aluminosilicate glasses (Sukenaga et al., 2017; Le Losq et al., 2017). To further consider the distribution of framework units and the violation of the Loewenstein's rule in aluminosilicate glasses, an extended modified random network (EMRN) model was proposed (Allu et al., 2018; Ganisetti et al., 2019). According to this model, three regions co-exist (figure 4): a depolymerized channel region (similar to MRN) and a SiO_4/AlO_4 network structure region that is separated in 'heteronuclear' (mainly Si-O-Al and Al-O-Al) and 'homonuclear' (mainly Si-O-Si) regions. M^{n+} cations acting as charge compensator favor the formation of Si-O-Al heteronuclear regions, whereas M^{n+} cations acting

as modifiers are associated with several Si-NBO forming depolymerized regions. The Si atoms in excess of Si-O-Al and Si-NBO bonds form SiO_4-rich 'homopolar' regions.

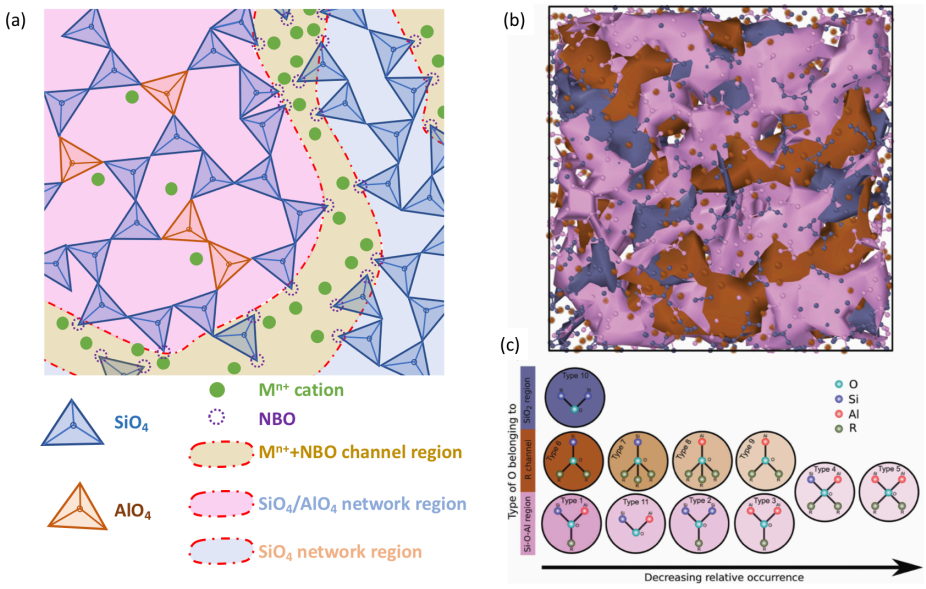

Figure 4. (a) Schematic 2D representation of the EMRN separating three regions in $M^{n+}{}_nO$-Al_2O_3-SiO_2 glasses (Allu et al., 2018; Ganisetti et al., 2019). (b) MD simulations of a (Ca,Mg)O-Al_2O_3-SiO_2 glass showing the SiO_4/AlO_4 network regions (pink), the SiO_4 network region (blue) and the alkaline-earth rich channels (brown). (c) Possible O environments with the background color corresponding to the three regions in (b); the intensity reflects the probability of occurrence of the O type in each region. Reprinted with permission from (Ganisetti et al., 2019). Copyright (2019) by the Royal Society of Chemistry.

Local environment around Al - Over coordinated Al

Al in tetrahedral coordination is predominantly present in aluminosilicate glasses as in most minerals, zeolites and ceramics. The aluminum environment has been investigated using many experimental techniques: Raman spectroscopy (Brawer, 1977; McKeown, 1984), X-ray absorption spectroscopy (McKeown, 1985; Landron et al., 1992; Wu, 1999; Sen, 2000; Neuville et al., 2004b; Moulton et al., 2016) and NMR (McMillan and Kirkpatrick, 1992; Stebbins, 2000; Toplis, 2000; Neuville et al., 2006).

The phase diagram of a $M_{2/n}O$-Al_2O_3-SiO_2 system (n= 1, 2) can be divided in two domains called peralkaline(-earth) for a ratio $R = M^{n+}/nAl > 1$ and peraluminous for a ratio $R = M^{n+}/nAl < 1$. The line R = 1 separating these two domains is called the "charge compensation" or "charge balanced" join" corresponding to tectosilicate compositions. In the peralkaline(-earth) field (R > 1), the

concentration of M^{n+} cations allows the full compensation of the charge deficit of each $(AlO_4)^-$ tetrahedron and Al^{3+}, stabilized in tetrahedral position, behaves as a network former similar to Si^{4+}. M^{n+} cations in excess relative to Al^{3+} play a network modifying role and introduce NBOs into the structure. When R decreases, the number of NBOs decreases and the glass network connectivity increases. In principle, when R = 1, no more NBOs should remain in the glass network, all Al^{3+} atoms are tetrahedrally coordinated and the network is fully connected. In the peraluminous domain (R < 1), a deficit in the number of charge compensators does not allow the stabilization of all AlO_4 tetrahedra. Consequently, higher coordinated species (five-fold coordination $^{[5]}$Al or six-fold coordination $^{[6]}$Al) or O triclusters can be present.

However, the emergence of high field NMR in the beginning of 2000's led to a reconsideration of this simple structural picture. The presence of NBOs for glasses along the charge compensation join has been detected by ^{17}O NMR (Stebbins and Xu, 1997). Furthermore, numerous high-resolution solid-state ^{27}Al NMR studies (Toplis, 2000; Neuville et al., 2004b; Lee et al., 2004; Neuville et al., 2006; Neuville et al., 2007; Allwardt, 2007; Neuville et al., 2008; Kelsey et al., 2008; Xue and Kanzaki, 2008; Iftekhar et al., 2012; Jaworski et al., 2012; Park and Lee, 2012; Park and Lee, 2014; Le Losq et al., 2014; Novikov et al., 2017) have inarguably revealed that aluminum is present in highly coordinated sites (i.e., five and six-fold coordination, $^{[5]}$Al and $^{[6]}$Al) even in the peralkaline(-earth) domain or along the charge compensation join (figure 5). The formation of $^{[5]}$Al is clearly favored over that of $^{[6]}$Al and both populations of $^{[5]}$Al and $^{[6]}$Al change with pressure, temperature, composition (Si/Al or M/Al ratios) or with the nature of M^{n+} cations. Aluminum coordination increases under static or dynamic compression, particularly in depolymerized glasses (Sato et al., 1991; Yarger, 1995; Lee, 2004; Lee et al., 2004; Allwardt et al., 2005a; Allwardt et al., 2005b; Kelsey et al., 2009; Lee, 2010; Bista et al., 2015). The effect of temperature has been studied *in situ* or by varying the quenching rate (Sato et al., 1991; Kanehashi and Stebbins, 2007; Florian, 2007; Stebbins et al., 2008; Thompson and Stebbins, 2013; Le Losq et al., 2014). The proportion of $^{[5]}$Al tend to increase with increasing temperature (*in situ* measurement) or fictive temperature (obtained when varying the quenching rate) but the variations are small compared to the effect of pressure. The fraction of $^{[5,6]}$Al sites strongly depends on the CFS of non-framework cations with high CFS favoring large population of $^{[5,6]}$Al (figure 6) (Neuville et al., 2008; Kelsey et al., 2008; Iftekhar et al., 2012; Jaworski et al., 2012). The higher content of $^{[5,6]}$Al is also observed for RE-aluminosilicate and Zn-aluminosilicate glasses but these cations seems to follow a different trend (Schaller and Stebbins, 1998; Florian, 2007; Iftekhar et al., 2012; Jaworski et al., 2012; Jaworski et al., 2015; Cormier et al., 2021).

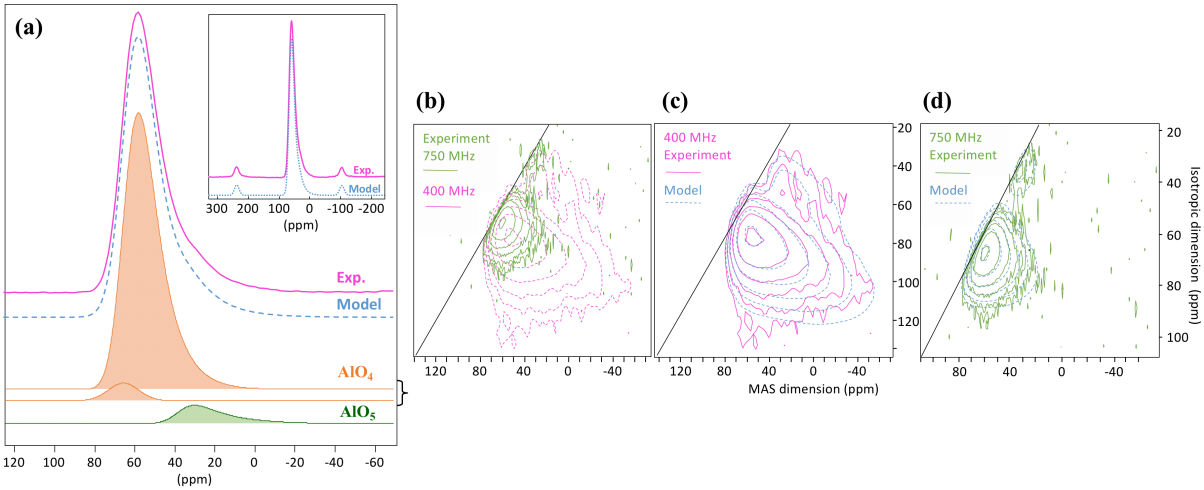

Figure 5. (a) ^{27}Al 1D NMR spectrum (750 MHz) of a CaO-Al_2O_3-2SiO_2 glass, showing the individual contributions of the $^{[4]}$Al and $^{[5]}$Al sites, including the spinning sideband of the satellite transition. The inserts show the experimental and simulated spectra (including central transition and first spinning sidebands of the outer transitions). (b) ^{27}Al 3Q MAS NMR spectra for the same glass measured at 400 Mhz (9.4T) and 750 MHz (17.6 T). (c) and (d) Comparison between the experimental spectra and the simulated spectra with the same fitting parameters for the two fields. Data from Neuville et al. (2004b).

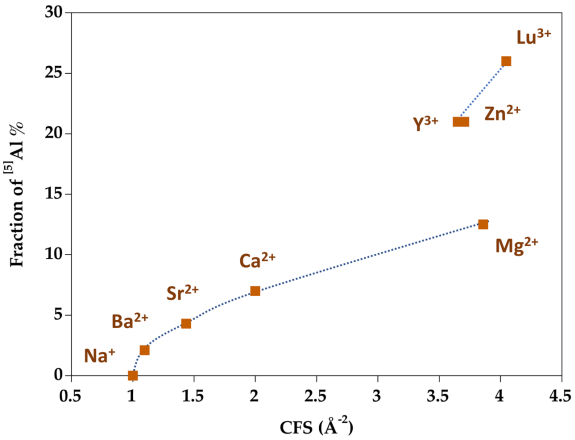

Figure 6. Changes in the fraction of $^{[5]}$Al with CFS for tectosilicate glasses with 50 mol.% SiO_2. Curves are only guide for the eye. Data from Neuville et al. (2006); Neuville et al. (2008); Iftekhar et al. (2012); Novikov (2017); Cormier et al. (2021).

The average cationic potential has been proposed to account for changes in $^{[5,6]}$Al fractions with composition (Park and Lee, 2014). The average cationic potential is the ratio of charge (c) to ionic radius (r) normalized by the mole fraction of each non-network cation:

$$\langle c/r \rangle_{ave} = \sum_i x_i \frac{c_i}{r_i}$$

where x_i, c_i and r_i are the mole fraction, the charge and the ionic radius of cation i, respectively. Park and Lee (2014) have summarized (figure 7) the population of $^{[5,6]}$Al as a function of $\langle c/r \rangle_{ave}$ in all the ternary or multi-component aluminosilicate glasses studied so far. The population of $^{[5,6]}$Al shows an increasing trend when $\langle c/r \rangle_{ave}$ increases. A threshold is observed at $\langle c/r \rangle_{ave} = 2$ with a significant increase of the fraction of $^{[5,6]}$Al above this value but with considerable dispersion. This is explained because, at a constant $\langle c/r \rangle_{ave}$, the population of $^{[5,6]}$Al strongly depends on both $M^{n+}O_{n/2}/Al_2O_3$ and Si/Al ratios (Neuville et al., 2006; Neuville et al., 2008; Kelsey et al., 2008; Thompson and Stebbins, 2012).

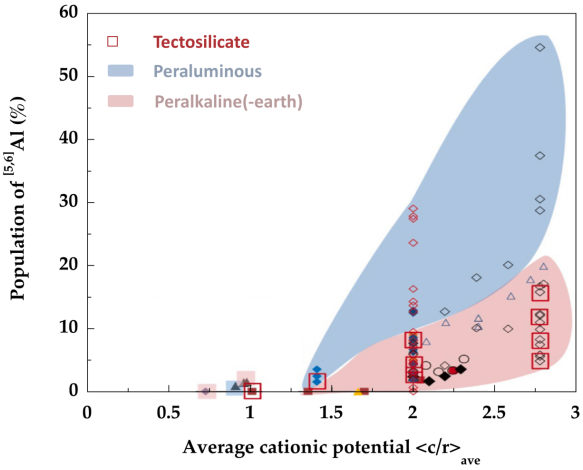

Figure 7. Change of the fraction of $^{[5]}$Al with the average cationic potential for various multicomponent aluminosilicate glasses. Modified from Park and Lee (2014). Copyright (2014) by Elsevier.

Each $(AlO_6)^{3-}$ octahedron is commonly considered as composed of three BOs and three NBOs (Day and Rindone, 1962) and has a network modifying character. Its content is always small compared to $^{[5]}$Al because packing requirements for octahedral Al are unfavorable (Lacy, 1963). Conversely, the structural role of $^{[5]}$Al as either a network former or a network modifier remains a fundamental debated question (Takahashi et al., 2015). Using MD simulations of Ca-AS glasses, the bond angle distributions of AlO_5 (and SiO_5) units have been analyzed (Wiles et al., 2020), revealing that $^{[5]}$Al and $^{[5]}$Si environments are consistent with the range of configurations found in a Berry pseudorotation (motion between two trigonal bipyramidal configurations). As $^{[5]}$Al sites adopt any environment between the two extreme geometries with a minimal energy cost, the presence of $^{[5]}$Al can likely play a governing role in mechanisms of plastic deformation or viscous flow. Similar to $^{[5]}$Si, $^{[5]}$Al could be a transient species, thermally activated, that facilitates the diffusion of NBOs and the

exchange of T-O bonds (Stebbins and Farnan, 1992; Farnan and Stebbins, 1994; Neuville et al., 2007). Increasing the fraction of higher coordinated species can help to explain low viscosity at high pressure and reduced viscosities at high temperature (Lee et al., 2004; Allwardt, 2007; Wiles et al., 2020). Furthermore, glasses with low hardness tend to have high $^{[5]}$Al fractions (Iftekhar et al., 2012; Stevensson and Edén, 2013; Lamberson, 2016), suggesting that higher coordinated species could improve mechanical properties.

Oxygen tricluster

As NBOs have been unexpectedly reported in compositions along the charge balancing joins (Stebbins and Xu, 1997), oxygen triclusters, O_{tri}, were proposed together with highly coordinated Al to maintain the network charge neutrality. By definition, O_{tri} is a special configuration of triply coordinated oxygen, $^{[3]}$O, only bonded to three tetrahedra (Figure 8a and b): one AlO_4 and two SiO_4 or two AlO_4 and one SiO_4 (for this latter case a charge compensator is required in close proximity to maintain charge neutrality). Oxygen atoms coordinated to three, highly charged, tetrahedral cations are in strongly energetic configurations and violate Zachariasen's rules as O atoms are bonded to three network formers. A tricluster configuration can be regarded as an Al^{3+} ion acting as a modifier ion and bonded to NBOs (figure 8c).

The presence of triclusters results in a more compact packing and, thereby, higher densities are expected (Toplis et al., 1997b). More importantly, triclusters can play a dominant role in transport properties, particularly for self-diffusion of oxygen in melts and viscous flow processes (Toplis et al., 1997b). However, their presence is still debated and their influence on properties not ascertained (Tandia et al., 2011). O_{tri} are mostly supported by MD simulations using classical (Cormier et al., 2003; Barbieri et al., 2004; Tandia et al., 2011; Bouhadja et al., 2014; Agnello et al., 2019) or *ab initio* approaches (Benoit et al., 2005). Experimentally, they have been detected only in a calcium aluminate glass using advanced NMR methods (Iuga et al., 2005).

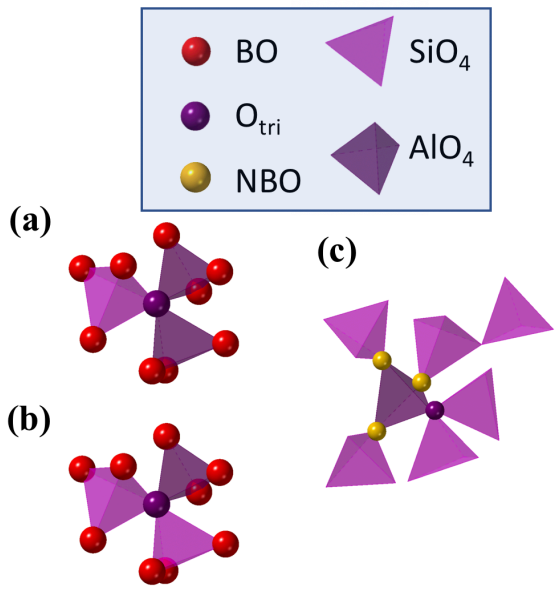

Figure 8. Common oxygen shared between three tetrahedra: (a) one SiO_4 and two AlO_4 or (b) one SiO_4 and two AlO_4. (c) Al^{3+} in tetrahedral environment, equivalent to (a), with one O tricluster (O_{tri}) and three NBOs in the first coordination shell.

The main aluminosilicate systems

Many different glasses can be obtained with aluminum and sometimes an extremely wide range of compositions can be achieved compared to the few crystalline compositions. Richet et al. (2006) have reviewed the glass forming regions in several important alkali/alkaline earth systems, showing a close connection between glass forming ability (GFA) and viscosity, low liquidus temperature and low configuration heat capacity. The main important families of glasses containing Al_2O_3 are documented in this part, by outlining the current structural knowledge in relation to physico-chemical properties.

Aluminate glasses

Binary aluminate glasses are remarkable materials as they are free of typical glass network forming oxides but contain a high proportion of alkaline-earth or RE oxides. They have excellent mechanical properties (Rosenflanz et al., 2004; Johnson et al., 2005; Rosales-Sosa et al., 2015; Rosales-Sosa et al., 2018), high softening points (Johnson et al., 2005) and some of the highest sound speeds of any glassy systems (Yeganeh-Haeri et al., 1998). Vickers hardness (H_v = 9.5 GPa) and elastic modulus (E = 158 GPa), reported for a $46Ta_2O_3$-$54Al_2O_3$ glass, are among the highest values among oxide glasses (Rosales-Sosa et al., 2015). Molten aluminates have viscosities that do not follow

an Arrhenius behavior and are thus classified as 'fragile' (Wallenberger and Brown, 1994; Weber et al., 1998). The fragility of these systems is related to a large configurational entropy as many structural states are available in liquids due to possible change in cationic environment.

Calcium aluminate (CA) glasses are attractive due to a promising infrared (IR) transparency up to $\lambda = 6$ µm (Hafner et al., 1958; Higby, 1990; Sung and Kwon, 1999), similar to sapphire. With small SiO_2 doping, they can have ultralow optical losses compared to pure SiO_2 (0.04 dB km^{-1} for a SiO_2-low CA glass compared to 0.16 dB km^{-1} for SiO_2 at 1.55 µm (Lines et al., 1989)). A high elastic modulus of 125 GPa was reached for a ZnO-CA glass-fiber (Wallenberger and Brown, 1994), higher than that of a S-glass (87 GPa) that is the high-strength glass-fiber exploited for reinforcement composites. Such properties make CA glasses of considerable technological value for diverse applications (laser windows, IR domes or windows, IR fiber optics (Wallenberger and Brown, 1994; Weber et al., 1998; Hwa, 1998). CA glasses are also important as analogue systems of metallurgical slags and hydraulic cements (Skibsted et al., 1993; Poe, 1994; Douy and Gervais, 2000).

CA glasses can be synthesized using a conventional furnace and quenching rate in a narrow range near the eutectic composition ($64CaO\text{-}36Al_2O_3$, CA36) (Sung and Kwon, 1999). A wider glass formation range (20-80 mol.% CaO) can be accessed using containerless methods such as aerodynamic levitation coupled with laser heating (McMillan and Piriou, 1983; Weber et al., 2002; Benmore et al., 2003; Neuville et al., 2010). A technique using solar furnace melting and splat quenching has allowed glasses with fast quenching rates of 10^6-10^7 K s^{-1} to be obtained (McMillan and Piriou, 1983; McMillan, 1996). The GFA of CA can also be enhanced by addition of various oxides, improving the glass stability and reducing the presence of hydroxyl bonds (Onoda and Brown, 1970; Shelby, 1989; Uhlmann, 1993; Shelby, 1995).

From Al_2O_3-poor glasses to the tectosilicate composition (CaO > 50 mol.%), tetrahedrally coordinated Al is the only species detected by high resolution ^{27}Al NMR and Raman spectroscopies, with no change whatever to the quenching rate (McMillan and Piriou, 1983; McMillan, 1996; Neuville et al., 2006; Neuville et al., 2010). Addition of CaO progressively disrupts the fully-connected network of AlO_4 tetrahedra in CA50 glass ($50CaO\text{-}50Al_2O_3$) and reduces the O coordination (Akola et al., 2013; Edén, 2015). The average oxygen coordination number (CN) around Ca is mainly determined by numerous X-ray and neutron diffraction studies and shows a rather wide range of values from 4 to 5.5 for similar CA compositions between CA30 and CA50 (Morikawa et al., 1983; Hannon and Parker, 2000; Cormier et al., 2000b; Mei et al., 2008a; Mei et al., 2008b; Drewitt et al., 2011; Benmore et al., 2003), probably due to an asymmetric distribution of O neighbors around Ca. MD simulations give a higher average CN of 6, with a wide range of distribution of Ca sites, for various CA glasses (from CA75 to CA25) (Kang et al., 2006; Thomas et al., 2006; Drewitt et al., 2011) but the choice of potentials appears to have a major influence on the estimation of CN for Al and Ca. The role of Ca is not clear but it was proposed that this cation behaves as a network former

together with Al (Benmore et al., 2003). Recently, by using a combination of DFT and RMC simulations, the CA36 glass has been described as a topologically disordered cage network with a wide ring size distribution and many large-sized rings (Akola et al., 2013). This structural organization differs from that of CA50 glass and could reflect the high GFA of glasses near the eutectic composition. When CaO ≤ 50 mol.%, high Al coordinated species $^{[5,6]}$Al and O_{tri} begin to appear (McMillan, 1996; Iuga et al., 2005; Neuville et al., 2006; Mei et al., 2008a) and these species can also be observed in MD simulations (Drewitt et al., 2011). Using $\{^{17}O\}\{^{27}Al\}$ HMQC (heteronuclear multiple quantum correlation) NMR experiments, the formation of ~5% O_{tri} has been evidenced in a CA50 glass (Iuga et al., 2005). Edge or face-sharing AlO_4 units could also be present in Al_2O_3-rich compositions based on specific Raman bands at ~620 cm^{-1} and 430 cm^{-1} (McMillan and Piriou, 1983).

Structural defects (for instance superoxide O_2^- ion radical or peroxy -O-O- linkages; see Hosono and Abe, 1987) appear to be very specific to CA glasses close to the eutectic and they could explain high photosensitivity to ultraviolet rays (Hosono et al., 1985). Quenching a CA37 melt in strongly reducing conditions has allowed the synthesis of an electride glass, C12A7:e^- (Kim et al., 2011), that contains stabilized solvated electrons trapped in cages of the CA network, which could give a potential glassy electronic conductor. Based on DFT-RMC simulations of CA37 glass, the structural origin of these solvated electrons was proposed to be due to efficient elemental mixing resulting from similar atomic charges for Al and Ca and a network cage structure resulting from considerable fraction of large-sized rings that can host solvated electrons (Akola et al., 2013). However, since the glass transition temperatures of C12A7:e^- glass (T_g = 973 K) radically differs from that of the oxidized glass (T_g = 1133 K) (Kim et al., 2011), fundamentally different structures can be alternatively expected (Edwards, 2011).

Other alkaline-earth glasses obtained using containerless techniques have been investigated: Ba and Ba-Ti aluminates (Skinner et al., 2006; Skinner et al., 2012), Ba and Sr aluminates (Alahrache, 2011; Licheron et al., 2011), showing glass forming regions in various ranges for Ba (33-37 and 62-75 mol.% BaO) and Sr (37-40 and 55-75 mol.% SrO). Only glasses with excess of alkaline-earth oxides have been investigated revealing the expected network of corner-sharing AlO_4 tetrahedra.

Rare-earth (RE) aluminates are another class of glasses of high interest due to their luminescence properties, offering potential applications, particularly in the field of white light-emitting diodes. The GFA of these compounds is low and they are mainly prepared using contactless conditions (Weber et al., 1998; Zhang and Navrotsky, 2004; Watanabe et al., 2012). According to Watanabe et al. (2012), RE aluminate glasses can be obtained between 0.20 < RE_2O_3 (mol.%) < 0.5 and all systems form glasses for 30-32 mol.% RE_2O_3. The glass forming region increases with the RE^{3+} ionic radius and is the widest for the La_2O_3-Al_2O_3 system (27-50 mol.%).

Y_2O_3-Al_2O_3 (YA) glasses have attracted special interest as a potential glassy laser host (similar to crystalline $Y_3Al_5O_{12}$ garnet, the so-called YAG) and as a system displaying a variety of non-

equilibrium phenomena (McMillan, 2003; McMillan, 2008). Yttrium aluminate glasses were synthesized in the range of 0.2-0.4 mol.% Y_2O_3 by aerodynamic levitation or in an iridium wire furnace (Tangeman, 2004; Skinner et al., 2008; Nasikas et al., 2011). YA glasses and their melts have been the subject of numerous studies due to the possible existence of polyamorphism in this system (Wilding, 2001; Wilding et al., 2002; Wilding and McMillan, 2002; McMillan, 2003; Tangeman, 2004; Weber et al., 2004; McMillan, 2008; Skinner et al., 2008; Greaves, 2008; Barnes, 2009; Greaves, 2009; Nasikas et al., 2011). Aasland and McMillan (1994) have observed the coexistence of two glassy states of identical composition but different structures, densities and thermodynamic properties (figure 9). Using differential scanning calorimetry, two glass transition temperatures were determined at ~1135 K and 1300 K and attributed to HDA (high density amorphous) and LDA (low density amorphous) states, respectively (Wilding, 2001; Wilding et al., 2002; Nasikas et al., 2011). The two glassy states were mechanically separated to determine their respective densities (3.72 and 3.58 g cm^{-3}), allowing the assignment of the HDA and LDA to the inclusions and the glass matrix, respectively (McMillan, 2008). Note that the assignment is surprising since single HDA glass can be formed, suggesting that it is the stable amorphous form, and several studies indicate LDA inclusions in the HDA glass matrix (Florian et al., 2001; Nasikas et al., 2011). The two HDA-LDA states imply a density-driven phase separation that could underline a first-order liquid-liquid phase transition. However the occurrence of this polyamorphism has been strongly debated (Greaves, 2008; Barnes, 2009; Greaves, 2009).

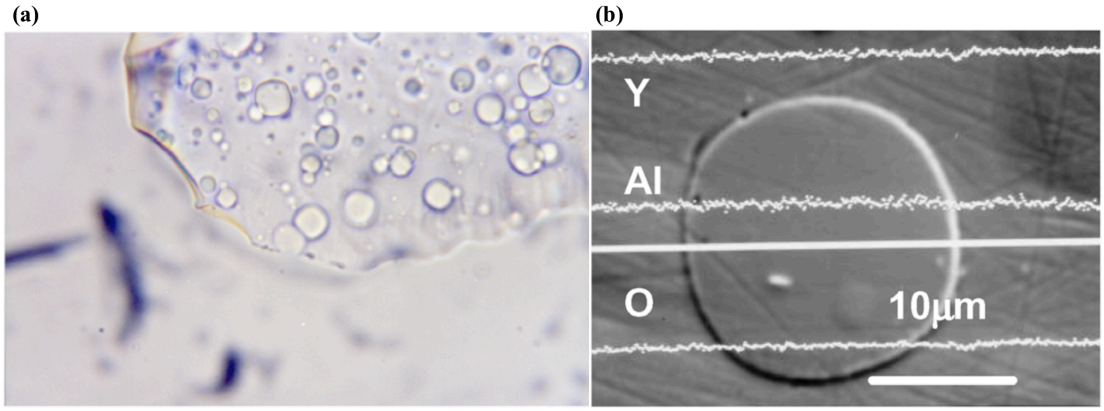

Figure 9. (a) Photomicrograph of a $23Y_2O_3$-$77Al_2O_3$ sample, showing sub-spherical glassy inclusions embedded within a glassy matrix. (b) Electron microprobe analysis for all elements (Y, Al, O) across a single inclusion. The lack of composition change at the inclusion-matrix interface indicates identical chemical compositions. Reprinted from McMillan (2008). Copyright (2008) by Elsevier.

Structural studies, using ^{27}Al and ^{89}Y NMR, Raman and diffraction, have been conducted mainly on Y_2O_3-Al_2O_3 and La_2O_3-Al_2O_3 glasses among RE_2O_3-Al_2O_3 glasses (Florian et al., 2001; Wilding, 2002; Wilding et al., 2002; Wilding and McMillan, 2002; McMillan, 2003; Weber et al., 2004; Tangeman, 2004; Nasikas et al., 2011; Watanabe et al., 2020), supported by MD simulations (McMillan, 2007; Du and René Corrales, 2007; Cristiglio et al., 2007; Du et al., 2009). Aluminum occurs predominantly in tetrahedral environment but, in La aluminate glasses, the population of $^{[4]}Al$ slightly increases with Al_2O_3 from 85% for 27 mol.% La_2O_3 to 94% for 50 mol.% La_2O_3 (Watanabe et al., 2020), while the fraction of $^{[4]}Al$ is essentially composition independent in YA glasses and has low values between 61% (Watanabe et al., 2020) and 69% (Tangeman, 2004). High coordinated Al species are detected in all Y- and La-aluminate glasses with rather large fractions of $^{[5]}Al$ (24-28%) and $^{[6]}Al$ (6-11%) in YA glasses (Watanabe et al., 2020; Tangeman, 2004). ^{27}Al 3Q-MAS reveals the presence of two different $^{[5]}Al$ environments in a YA glass with 37.5 mol.% Y_2O_3, supporting a phase separation (Florian et al., 2001) but this was not confirmed in further investigations (Tangeman, 2004; Nasikas et al., 2011). Diffraction results indicate an average CN of 7 oxygen atoms around La (Weber et al., 2004), as confirmed by MD simulations (Du and René Corrales, 2007). The Y-O distance distribution is asymmetric with distorted six and seven-fold polyhedra ($^{[6]}Y$ and $^{[7]}Y$) (Wilding, 2002; Wilding et al., 2002; McMillan, 2003; Du et al., 2009). Using ^{89}Y NMR, two distinct sites have been evidenced and interpreted as $^{[8]}Y$ and possibly $^{[9]}Y$ (Nasikas et al., 2011). They were associated with different Y environments in the LDA and HDA (Nasikas et al., 2011). An increase in the Y coordination number with increasing Al_2O_3 content emerges based on diffraction and NMR data (Weber et al., 2004; Nasikas et al., 2011). Several conclusions on the polyamorphic transition have been obtained from diffraction results (figure 10). Minor changes occur in the local Al environment (Wilding, 2002) contrary to the local Y environment that changes from $^{[7]}Y$ to $^{[8]}Y$ with the formation of LDA (Weber et al., 2004). This is accompanied by a high-degree of medium range order in glasses with amorphous-amorphous separation, similar to that in La aluminate glasses (Wilding, 2002). These changes at medium range distance indicate specific packing among AlO_n and YO_n units as revealed by metal-metal distances (Wilding, 2002; Wilding et al., 2002; McMillan, 2003; Weber et al., 2004). These modifications can be ascribed to a shift from corner to edge sharing between polyhedra as the Y coordination increases (Weber et al., 2004). MD simulations confirm that changes in the Y-Y correlations is the main difference between HDA and LDA configurations (McMillan, 2003). Furthermore, dynamic density fluctuations have been evidenced in MD simulations (McMillan, 2007), confirming experimental indication of unmixing of high and low density liquids at the nanoscale that underlines a liquid-liquid phase transition (Greaves, 2008; Greaves, 2009).

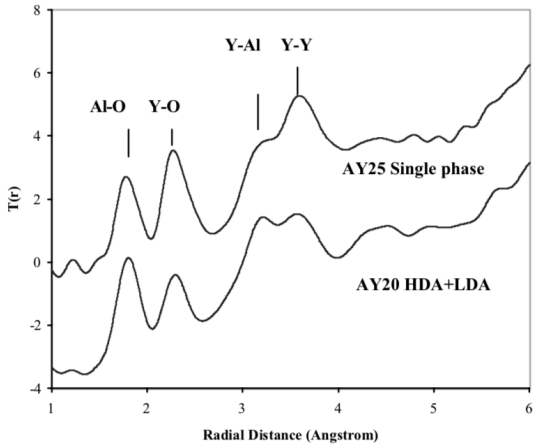

Figure 10. X-ray total pair-correlation functions for a single-HDA glass (AY25 = $25Y_2O_3$-$75Al_2O_3$) and a two-phase HDA-LDA glass (AY20 = $20Y_2O_3$-$80Al_2O_3$). The Al-O peak remains unchanged on transition from HDA to LDA. Conversely, there is an increase in the Y-O distance and in mid-range order (especially the peak ascribed to Y-Y correlations) in the HDA suggesting higher numbers of corner-shared AlO_n-YO_n polyhedra and edge-shared YO_n-YO_n polyhedra. Reprinted from Wilding et al. (2002). Copyright (2002) by Elsevier.

Compared to conventional silicate glasses, RE aluminate glasses have high hardness, high elastic moduli, and high cracking resistance *CR*, depending on the RE^{3+} ionic radius, r_{RE}. Increasing r_{RE} yields a decrease in packing density, elastic moduli and hardness and an increase in *CR* (Rosales-Sosa et al., 2018). The proposed mechanism underlying this high *CR* is the possibility for aluminum to adopt diverse coordination environments. This flexibility is higher than in silicate glasses, for which only SiO_4 tetrahedra are possible, and favors a stress release during plastic deformation. Large r_{RE} (e.g. for La) enhances the flexibility of the glass network compared to small r_{RE} (e.g. for Y). Indeed, Al in tetrahedral environment exists in large fractions in La_2O_3-Al_2O_3 glasses and these $^{[4]}Al$ are available to increase their oxygen CN under applied stress, whereas $^{[5]}Al$ and $^{[6]}Al$ species already exist in significant proportions in Y_2O_3-Al_2O_3 glasses so that a local Al change is difficult, associated with a high packing density that reduces densification ability.

Comparing RE^{3+} and M^{2+} aluminate glasses, Watanabe et al. (2020) have shown that above a packing density of ~55%, the network cannot accommodate only AlO_4 units. The less efficiency of RE^{3+} cations compared to M^{2+} cations for charge compensation of $(AlO_4)^-$ tetrahedra is related to the high CFS of RE^{3+} cations. RE^{3+} cations attract oxygen atoms more strongly than M^{2+} cations, bringing AlO_4 polyhedra closer to each other and increasing the packing density. Ideally, each RE^{3+} should charge balance three AlO_4 tetrahedra, which is topologically difficult if corner-sharing is maintained.

Al_2O_3-SiO_2 binary glasses

Replacement of silicon by aluminum has been investigated in the Al_2O_3-SiO_2 (AS) binary system. Materials with high alumina content are considered for refractories and small amounts of Al_2O_3 help to homogenize the distribution of RE in optically active devices (Lægsgaard, 2002; Weber et al., 2008). Alumina-rich AS glasses, particularly at the mullite composition, $3Al_2O_3$-$2SiO_2$, have remarkable high hardness and high indentation cracking resistance with an elastic modulus as high as 134 GPa (Rosales-Sosa et al., 2016). The liquids along the Al_2O_3-SiO_2 join cover a wide range of viscosity-temperature behavior, from strong (SiO_2-rich) to fragile with increasing Al_2O_3 contents (Wilding et al., 2010). There is a wide metastable immiscibility gap in the AS binary, starting above 5 mol.% Al_2O_3 and finishing below 60 mol.% Al_2O_3, i.e. near the mullite composition (Macdowell and Beall, 1969; Risbud and Pask, 1977; Risbud, 1982). Though homogeneous glasses are difficult to prepare due to high viscosities for undercooled melts and the tendency to phase separate, they can be prepared using fast-quenching techniques (contactless, flame-spraying, roller-quenching …) or via a sol-gel route.

The structure of AS glasses was studied from SiO_2 containing Al_2O_3 impurities up to 67 mol.% Al_2O_3, mainly in relation to Al speciation. At very low Al_2O_3 contents, $^{[4]}$Al is the most dominant species but distorted $^{[6]}$Al and a minor amount of $^{[5]}$Al is also present (Poe et al., 1992; Sen and Stebbins, 1995; Sen and Youngman, 2004). The mechanisms of charge compensation for $(AlO_4)^-$ is still not clear. Oxygen triclusters (Lacy, 1963; Macdowell and Beall, 1969; Schmücker, 1997; Schmücker and Schneider, 2002), O vacancies (Lægsgaard, 2002), interstitial Al atoms in the network (Day and Rindone, 1962; Lægsgaard, 2002) or three-coordinated Al ($^{[3]}$Al) (Brower, 1978; Brower, 1979) have been proposed. While the existence of O_{tri} is still debated due to the difficulties to have experimental signatures, computational simulations agree with their formation (Winkler et al., 2004; Tossell and Horbach, 2005). The presence of O_{tri} induces a tightening and densification of the silicate network, increasing the glass stiffness. They have been invoked to favor phase separation and initiate crystallization (Macdowell and Beall, 1969; Schmücker and Schneider, 2002), though structural homogeneity has been suggested at molecular scales (Ando et al., 2018). MD models have shown substantial fractions of $^{[3]}$Al, for instance ~38% at 5 mol.% Al_2O_3 (Poe et al., 1992) but limited experimental evidence for such species exist (Brower, 1978; Brower, 1979). Addition of Al_2O_3 results in the rapid disappearance of 3- and 4-membered rings and increases disorder (Okuno, 2005; Ando et al., 2018).

At higher Al_2O_3 content (>4 mol.%), the three coexisting $^{[4,5,6]}$Al species were observed in numerous experimental investigations with somewhat contradictory results (Morikawa et al., 1982; Risbud et al., 1987; Sato et al., 1991; Poe et al., 1992; Sen and Youngman, 2004; Okuno, 2005; Weber et al., 2008; Wilding et al., 2010; Ren et al., 2014). A peak at 30 ppm in ^{27}Al NMR spectra, usually

assigned to $^{[5]}$Al, is sometimes attributed to a distorded triclustered $^{[4]}$Al configuration (Schmücker and Schneider, 1996; Schmücker and Schneider, 2002). However, the main observed trend is that $^{[4,5]}$Al are the dominant species and $^{[6]}$Al persists but in small fractions. A recent ^{27}Al NMR investigation concludes with the absence of significant compositional dependence, even in phase separated glasses, up to 28 mol.% Al_2O_3, and only Si-O-$^{[4,5]}$Al and Si-O-Si linkages are detected with no Al-O-Al linkages (Sen and Youngman, 2004). The concentration of $^{[5,6]}$Al species increases upon further addition of Al_2O_3 (up to 60 mol.% Al_2O_3) (Risbud et al., 1987) and $^{[5]}$Al becomes the predominant species (Weber et al., 2008; Hoang, 2007). The exact Al speciation appears to depend on the synthesis conditions and quenching rates (Sato et al., 1991; Poe et al., 1992; Okuno, 2005; Ren et al., 2014). For instance, at a slow quench rate, there is no $^{[5]}$Al and only the presence of $^{[4]}$Al and $^{[6]}$Al species is observed (Sato et al., 1991; Poe et al., 1992). MD simulations indicate large fractions of $^{[3]}$O (and not O_{tri} as inaccurately stated in the papers) that are bonded to two edge-shared AlO_n polyhedra and an additional corner-shared AlO_4 or SiO_4 tetrahedron (Winkler et al., 2004; Pfleiderer, 2006; Hoang, 2007; Hoang, 2007). From diffraction data, an average low Al-O-T angle of 125° has also been interpreted as edge-shared AlO_n polyhedra in addition to corner-shared units (Weber et al., 2008). Such a configuration indicates a locally dense region and implies Al clustering that could prefigure phase separation. Proximity between all $^{[4,5,6]}$Al units has been confirmed by advanced NMR techniques (Ren et al., 2014). As the packing density increases with addition of Al_2O_3, the elastic moduli and Vickers hardness increase. The improved elastic properties are probably due to the flexibility for Al to adapt its environment to stresses (Rosales-Sosa et al., 2016). MD simulations indicate that indentation results from a shear deformation process at high Al_2O_3 content (Luo et al., 2016). The increasing glass ductility with increasing Al_2O_3 content is caused by a high proportion of high-coordinated Al that prevents the formation of defects acting as weak spots during deformation.

Alkali aluminosilicate glasses

Alkali-bearing aluminosilicate glasses have wide applications, such as chemically strengthened cover glasses or precursors for glass-ceramics. Na_2O-Al_2O_3-SiO_2 (NAS) glasses have attracted attention due to non-monotonic changes in physical properties, such as refractive index, density, viscosity and electrical conductivity (Day and Rindone, 1962; Riebling, 1966; Toplis et al., 1997a; Toplis et al., 1997b). Viscosity measurements have shown a particularly interesting behavior (figure 11) (Riebling, 1966; Toplis et al., 1997a; Toplis et al., 1997b): at a constant SiO_2 content, viscosities increase when Al substitutes for Na (ratio R = Na/Al < 1) with a maximum near R = 1 or slightly in the peraluminous region (R = 1.2) and then decreases slightly in the peraluminous region (R > 1). A similar behavior is also reported for Li_2O-Al_2O_3-SiO_2 (LAS) glasses (Shelby, 1978). In the peralkaline

region, the Al environment has been confirmed to be only tetrahedral by ^{27}Al NMR experiments (Lee and Stebbins, 2000b; Allwardt et al., 2005b), consisting of Q^4 species and conferring a pure network forming role on Al (Gambuzzi et al., 2014). Only $^{[4]}$Al is also detected in KAS glasses (Thompson and Stebbins, 2011; Le Losq et al., 2017). The extremum in viscosity and its occurrence slightly in the peraluminous region has been strongly debated. This anomaly has not yet been truly understood since it can be attributed to the formation of O_{tri} or Al in high coordination states (Lacy, 1963; Riebling, 1966; Toplis et al., 1997b).

Experiments have failed to evidence the presence of O_{tri} because either this moity in glasses does not exist or is not present in significant amounts or current experiments are unable to identify it. For instance, the ^{17}O NMR signature of O_{tri} is predicted to fall in the range of chemical shifts for regular BO (Kubicki, 2002). Alternatively, MD simulations usually have significant contents of O_{tri} (typically 1-10%) (Xiang et al., 2013). The identification of O_{tri} can be an artefact due to fast quenching rates in simulations and, as such, MD models are more representative of a high temperature structure similar to that prevailing in viscosity measurements.

An increase in $^{[5]}$Al concentration would contribute to a decrease in viscosity (Toplis and Dingwell, 2004) and five-fold coordinated species are considered to be involved in the viscous flow of the network, promoting the exchange of T-O-T links (Farnan and Stebbins, 1994; Stebbins and Farnan, 1992). Their influence is expected to be more important for compositions with very polymerized networks, such as silica or albite, $NaAlSi_3O_8$, melts.

The presence of $^{[4]}$Al-O-$^{[4]}$Al linkages is negligible in the peralkaline region but tends to increase for compositions close to R = 1 (Lee and Stebbins, 1999; Lee and Stebbins, 2009). The values of glass transition temperatures (T_g) steeply increase near R = 1, which is explained as changes of the Si speciation from $Q_{Si}^3(0Al)$ to $Q_{Si}^4(mAl)$ units based on Raman spectroscopy (Le Losq et al., 2014). In the peraluminous region, the fraction of $^{[5]}$Al increases and the structure has been considered to be more constrained than for tectosilicate compositions as a result of ring statistics close to a 'perfect' six-membered ring distribution (Le Losq et al., 2014). It was concluded that the presence of $^{[5]}$Al in peraluminous glasses strongly impacts the rheologic and thermodynamic properties.

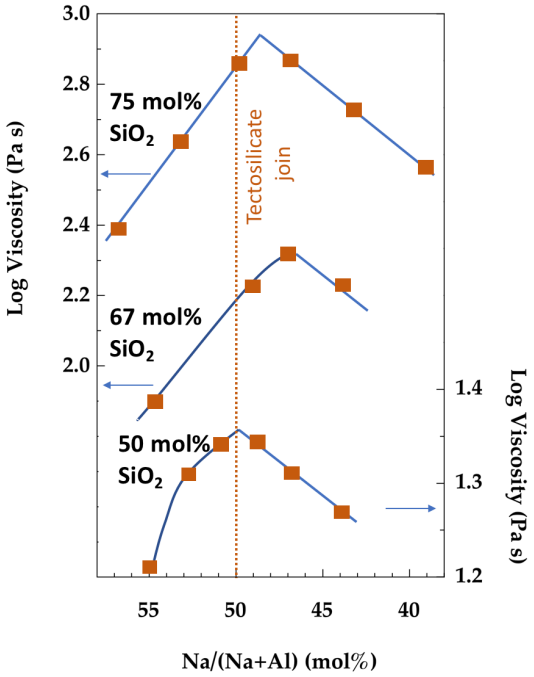

Figure 11. Experimental viscosities at 1869 K in Na-AS glasses with different SiO_2 contents as a function of Na/(Na+Al). Data from Toplis et al. (1997b).

Li_2O-Al_2O_3-SiO_2 (LAS) glasses have considerable importance as they are the precursors for most of commercialized glass-ceramics. They have also been considered due to the fast Li mobility and the potential development of solid-state electrolytes for ionic batteries (Pechenik et al., 1986; Pechenik et al., 1988; Greaves and Ngai, 1995a; Greaves and Ngai, 1995b; Ross et al., 2015). Similar observations on the conductivity properties were obtained for LAS and NAS (Li and Garofalini, 2004; Zirl and Garofalini, 1990). The initial introduction of Al_2O_3 blocks the alkali channels existing in the MRN model, increasing the activation energy for diffusion (Greaves and Ngai, 1995a). With further addition of Al_2O_3, a large fraction of alkalis changes their structural role, from modifying, associated with NBOs, to charge balancing near $(AlO_4)^-$ units, associated with BOs in Si-BO-$^{[4]}$Al bonds. Alkalis become loosely bounded due to large M^+-BO bond lengths and small M^+-BO binding energies compared to M^+-NBO bonds. As a result, the activation energy decreases as M^+-BO bonds are formed and is the smallest for $M^+/Al = 1$ (figure 12) (Li and Garofalini, 2004; Zirl and Garofalini, 1990). The formation of $^{[5,6]}$Al species for $M^+/Al < 1$ decreases the activation energy, following a reduction of the free volume. Li atoms are found in distorted tetrahedral sites that share edges with TO_4 tetrahedra (Cormier, 1998; Cormier, 2001). Due to Si/Al ordering, AlO_4 units are homogeneously distributed in the network, explaining large inter-alkali distances in AS glasses (Cormier, 1998; Cormier, 2001; Greaves and Ngai, 1995a). The proposed mechanism for alkali diffusion is a hopping process from a $(AlO_4)^-$ unit to another $(AlO_4)^-$ unit, provided by a higher free volume than for crystalline counterparts.

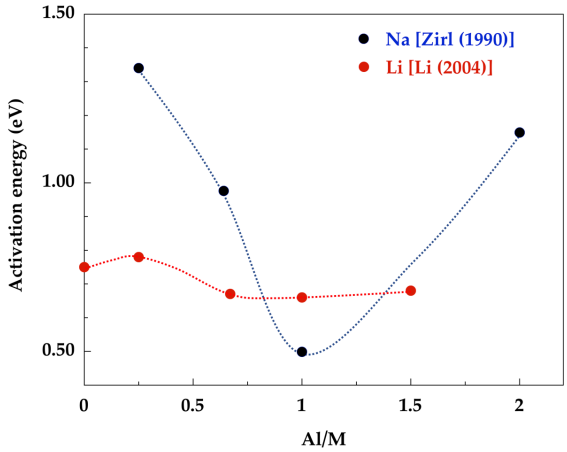

Figure 12. Variation of the activation energy of alkali diffusion as determined by MD simulations in Na and Li AS glasses as a function of Al/M content (M = Li or Na). Curves are only guides for the eye. Data from Zirl and Garofalini (1990) and Li and Garofalini (2004).

Alkaline-earth aluminosilicate glasses

Alkaline-earth aluminosilicate glasses exhibit interesting optical and mechanical properties and form the basis of a plethora of commercial glasses from nuclear, domestic and industrial waste storage, slags, cements, fibers, and industrial glasses.

GFA in the CaO-Al_2O_3-SiO_2 (CAS) system is remarkable since low-SiO_2 glasses can be formed, allowing compositions to be studied along the almost complete $R = CaO/Al_2O_3$ joins. Strong non-linear behavior has been observed for T_g (Higby, 1990; Cormier et al., 2005): a minimum at 30-40 mol.% SiO_2 along the join $R = Ca/2Al = 1$ and at 50-60 mol.% SiO_2 along the joins $R = 1.57$ and 3; for these two latter, an additional maximum at 10-20 mol.% SiO_2 is also observed. These observations have motivated numerous studies, especially on the connectivity of the tetrahedral aluminosilicate network. A large structure database exists for CAS based on various experimental and modeling techniques (Murdoch, 1985; Engelhardt et al., 1985; Merzbacher, 1991; Himmel, 1991; Stebbins and Xu, 1997; Petkov, 2000; Cormier et al., 2000b; Lee and Stebbins, 2000b; Allwardt, 2003; Stamboulis et al., 2004; Neuville et al., 2006; Lee and Stebbins, 2006; Neuville et al., 2007; Moesgaard et al., 2010; Thompson and Stebbins, 2011; Tandia et al., 2011; Jakse et al., 2012; Zheng et al., 2012; Thompson and Stebbins, 2012; Bouhadja et al., 2014) to determine the topological disorder, coordination numbers, bond-angle distribution, linkages between polyhedra and fulfillment of the aluminum avoidance principle. From these investigations, a general structural picture emerges that changes with R and SiO_2 content. Near pure SiO_2, the glass structure is composed of a fully connected network of corner-shared TO_4 tetrahedra and the addition of CaO progressively depolymerizes the network. Al^{3+} cations preferentially replace Si^{4+} cations in tetrahedral positions with Ca^{2+} charge

balancing two $(AlO_4)^-$ tetrahedra. Additionally, Al atoms prefer to occupy fully polymerized Q^4 sites and NBOs are almost entirely associated with Si atoms (Engelhardt et al., 1985; Allwardt, 2003). High coordinated Al polyhedra are expected only for insufficient modifier contents. However, a substantial fraction of $^{[5]}$Al species and minor amounts of $^{[6]}$Al species are present throughout the CAS ternary system, except at high SiO_2 content and for the low silica percalcic region (SiO_2 < 16 mol.%) (figure 13). The maximum $^{[5,6]}$Al fraction is observed near 40 mol.% SiO_2 for all joins in the percalcic region with a maximum of 7-8% $^{[5]}$Al (Neuville et al., 2006; Neuville et al., 2007). The presence of these high-coordinated species implies higher amounts of NBOs and $^{[3]}$O and non-negligible fractions of NBOs are observed along the charge-balanced join (Stebbins and Xu, 1997; Lee and Stebbins, 2006; Stebbins et al., 2008). Ca is acting both as a modifier and as a charge compensator and is localized in distorted sites with 6-7 oxygen neighbours, within interstitial spaces of the tetrahedral network (Cormier et al., 2003; Neuville et al., 2004a; Mongalo et al., 2016). The Al avoidance principle is violated and a quasi-heterogeneous distribution of Al as second neighbours around Si was proposed (Moesgaard et al., 2010). This model suggests the existence of depolymerized Si-NBO-Ca regions and highly polymerized regions of alternating SiO_4-(1/2Ca)AlO_4 units. MD simulations suggest spatial correlation between $^{[5]}$Al and $^{[3]}$O within small 2- and 3-fold membered rings (Benoit et al., 2005; Agnello et al., 2019; Atila et al., 2019). As the SiO_2 content decreases below 40 mol.%, Al atoms enter depolymerized Q^3 and Q^2 units and the number of NBOs per SiO_4 tetrahedron decreases (Neuville et al., 2006; Neuville et al., 2007; Bouhadja et al., 2014), forming a highly depolymerized network. The lower network connectivity of Al_2O_3-rich glasses increases the reactivity, which is crucial for developing supplementary cementitious materials (Nie et al., 2020). The presence of NBOs and their distribution on Si and Al units are correlated with the evolution of T_g and the fragility behavior of the corresponding melts. For peraluminous glasses, large proportions of $^{[5]}$Al exceeding 20% are observed but these compositions have been little investigated (figure 13b) (Neuville et al., 2006; Neuville et al., 2007). It has been suggested that non negligible fractions of NBOs are still present within the peraluminous region (Mysen and Toplis, 2007; Thompson and Stebbins, 2011).

The MgO-Al_2O_3-SiO_2 (MAS) system has a reduced GFA but the glass structure follows the general trends observed for CAS (McMillan and Kirkpatrick, 1992; Toplis, 2000). The main difference from their CAS counterparts is that higher fractions of $^{[5,6]}$Al species are detected in MAS glasses (figure 13) (Neuville et al., 2008). Divalent cations have thus a lower ability to stabilize $^{[4]}$Al than monovalent alkali cations. The average CN for Mg is close to 5 with a distribution between 4-, 5- and 6-fold coordinated sites (Guignard and Cormier, 2008; Mongalo et al., 2016). Therefore, owing to its small size and its localization in interstitial sites of the aluminosilicate network, Mg^{2+} cations perturb the network more severely than Ca^{2+} cations (Navrotsky, 1982; Roy and Navrotsky, 1984) and the network distortion can result in the formation of high-coordinated Al. Furthermore, the high CFS for Mg^{2+} favors the stabilization of more concentrated negative charges on NBOs or partially charged

BOs involved in $^{[4]}$Al-O-$^{[4]}$Al linkages. These different influences of Mg^{2+} and Ca^{2+} on the glass structure impact the macroscopic properties (density, Young's modulus, Vickers hardness, coefficient of thermal expansion, liquid fragility) (Smedskjaer et al., 2013).

In mixed Ca-Mg aluminosilicate glasses (CMAS), the fraction of $^{[5]}$Al species increases with MgO content and is less affected by the Si/Al or M^{2+}/Al substitutions (Lee et al., 2005; Neuville et al., 2008; Kelsey et al., 2008; Nie et al., 2020). The network polymerization depends mainly on the content of alkaline-earth ions and to a much lesser extent on the Al/Si and Mg/Ca substitutions (Nie et al., 2020). The degree of Si-Al disorder (presence of $^{[4]}$Al-O-$^{[4]}$Al) increases with the presence of Mg^{2+} cations and increasing Al/Si ratio (Lee et al., 2005; Kelsey et al., 2008). NBOs have more Mg^{2+} cations in their environment than Ca^{2+} cations. These latter cations are thus more associated with Al-O-Si linkages and slightly more available than Mg to charge balance $(AlO_4)^-$ units (Kelsey et al., 2008). This result is consistent with MD simulations indicating that more Ca ions are acting as charge compensator than Mg (Allu et al., 2018; Ganisetti et al., 2019). The non-random distribution of framework and non-framework cations supports the EMRN model implying an heterogeneous network (figure 4).

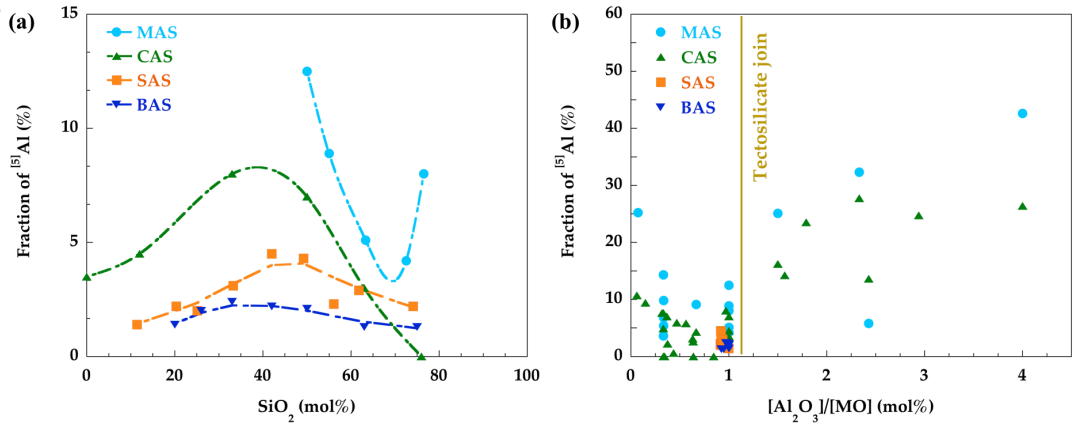

Figure 13. Comparison of the $^{[5]}$Al fraction in tecto-aluminosilicate glasses containing alkaline-earth cations (MAS: Mg^{2+}; CAS: Ca^{2+}; SAS: Sr^{2+}; BAS: Ba^{2+}) (a) as a function of the SiO_2 content (curves are guides for the eye) or (b) as a function of the ratio Al_2O_3/MO. Data from Neuville et al. (2006), Neuville et al. (2008), Novikov et al. (2017) and Novikov (2017).

Mechanical properties have been explored in CAS and MAS glasses (Smedskjaer et al., 2012; Veit and Rüssel, 2016), showing that increasing Al_2O_3 content provokes higher atomic packing density, responsible for higher values of Poisson ratio and that CFS has a high impact on elastic moduli. In CAS and MAS glasses, hardness shows an 'anomalous' behavior with a minimum (at ~85 mol.% SiO_2 for CAS and ~70 mol.% SiO_2 for MAS) and has higher values for MAS over CAS glasses

(Lamberson, 2016). As the hardness correlated with the proportion of $^{[5]}$Al + $^{[6]}$Al (R^2 = 0.9-0.91), Lamberson (2016) proposed that the presence of $^{[5,6]}$Al prevents the Ca-O bond breaking and reforming, this latter mechanism causing NBO motion and creating shear deformation. Indeed, NBOs are tightly held by $^{[5,6]}$Al since edged-shared $^{[5,6]}$Al-$^{[4]}$T bonds are stronger than $^{[4]}$T-$^{[4]}$T ones. $^{[5,6]}$Al ties up the structure and is beneficial for better crosslinking network fragments. Therefore, $^{[5,6]}$Al can prevent or slow down plastic deformation, and consequently hardness is increased. In addition to larger amounts of $^{[5,6]}$Al in MAS glasses, Mg-NBO bonds are stronger than Ca-NBO bonds and NBOs have thereby a lower ability to move in a MAS network over a CAS network, such that shear deformation is further inhibited. The different hardness behavior between the two alkaline earth cations is related to both higher proportion of $^{[5,6]}$Al and stronger Mg-NBO bonds. The fraction of $^{[5,6]}$Al has then a prominent role in controlling mechanical properties (shear deformation and hardness) of tectosilicate glasses with SiO_2 < 85 mol.%.

Other alkaline-earth AS glasses have been investigated less though the structure of Sr and Ba AS glasses have been explored (Thompson and Stebbins, 2012; Novikov et al., 2017; Charpentier et al., 2018). The substitution of Si by $SrAl_2O_4$ favors the formation of small-size rings. A CN for Sr near 6 was determined using an advanced diffraction investigation (Cormier, 1999), while a CN of 9 was proposed based on a crude fingerprint XANES approach (Novikov et al., 2017) and MD simulations indicate a broad distribution with maximum at ~7-8 (Charpentier et al., 2018). The proportion of $^{[5]}$Al is smaller (< 5%) for Sr^{2+} and Ba^{2+} than for Ca^{2+} and Mg^{2+} (figure 13), thus following the trend Ba < Sr < Ca < Mg that suggests an important size effect for these divalent cations (Thompson and Stebbins, 2012).

Rare-earth aluminosilicate glasses

Glass formation (Makishima et al., 1978; Makishima et al., 1982; Hyatt and Day, 1987; Shelby, 1994; Clayden et al., 1999; Iftekhar et al., 2011; Pahari et al., 2012) and the thermodynamic behavior (Zhang and Navrotsky, 2003; Zhang and Navrotsky, 2004) have been investigated in RE-based aluminosilicate glasses (RE-AS). The presence of trivalent RE cations (Sc^{3+}, Y^{3+} and lanthanides) in AS glasses leads to useful physico-chemical and mechanical properties: high refractive index, hardness and elastic modulus, low corrosion. RE-AS glasses are refractory with high T_g values (T_g > 840°C) and high chemical stability (Hyatt and Day, 1987; Shelby, 1990; Tanabe et al., 1992; Johnson et al., 2005). Most glass properties depend on the cation mass and CFS with the noticeable exception of Sc-bearing glasses that show anomalously low T_g values, possibly related to Sc clustering (Iftekhar et al., 2011). The density, refractive index, thermal expansion coefficient, microhardness, electrical resistivity all increase with the addition of RE oxides (Makishima et al., 1978; Shelby, 1994; Johnson

et al., 2005; Pahari et al., 2012). Decreasing the ionic size increases the elastic moduli and the thermal expansion coefficient (Shelby, 1990; Inaba et al., 2000; Tanabe et al., 1992). Owing to high refractive indices, they exhibit excellent optical properties and they can be used in technological applications, such as components in lenses, optical amplifiers, laser hosts, fiber optics. They have also been considered as potential matrices for storage of radioactive wastes (Bardez et al., 2005; Loiseau and Caurant, 2010; Kidari et al., 2012) and explored in radiotherapy for *in situ* cancer treatment (Christie and Tilocca, 2010a; Christie and Tilocca, 2010b). Addition of Al_2O_3 is beneficial to obtain homogeneous glasses with high contents of uniformly dispersed RE^{3+}cations.

RE-AS glasses have pronounced configurational and chemical disorder compared to alkaline or alkaline-earth AS glasses. Whereas tetrahedral coordination is still dominant, large amounts of $^{[5,6]}$Al populations prevail throughout the entire range of RE-AS glass forming regions (Jaworski et al., 2015; Schaller and Stebbins, 1998; Florian, 2007; Iftekhar et al., 2011; Jaworski et al., 2012; Iftekhar et al., 2012; Pahari et al., 2012; Okhotnikov et al., 2013), with larger amounts compared to mono/divalent cations. The relative amounts of $^{[5,6]}$Al grow with decreasing SiO_2 content (Florian, 2007; Iftekhar et al., 2012; Jaworski et al., 2012) and increasing CFS (Schaller and Stebbins, 1998; Florian, 2007; Iftekhar et al., 2011; Jaworski et al., 2012; Pahari et al., 2012) and depends on the RE/Al ratio:

- when RE/Al < 3, not enough RE^{3+} cations are present to ensure charge neutralization of $(AlO_4)^-$ groups and the highest amounts of $^{[5]}$Al (35%) and $^{[6]}$Al (5%) are observed (Schaller and Stebbins, 1998; Florian, 2007; Pahari et al., 2012);
- when RE/Al ≥ 3, $^{[4]}$Al is predominant with small fractions of $^{[5,6]}$Al and RE cations act as modifiers, depolymerizing the network with the formation of NBOs preferentially localized on SiO_4 tetrahedra (Lin et al., 1996; Schaller and Stebbins, 1998).

The higher coordinated $^{[5,6]}$Al species imply a significant cross-linked AS network that, is suggested, explains the enhanced Vickers hardness with increasing CFS (Iftekhar et al., 2012; Stevensson and Edén, 2013). A pronounced Al/Si atomic disorder (violation of Al avoidance principle) is observed based on NMR results (Iftekhar et al., 2009; Jaworski et al., 2012), as well as MD simulations (Jaworski et al., 2012; Okhotnikov et al., 2013). Even for SiO_2-rich glasses, in contrast to mono/divalent cations, NBOs directly connected with $^{[n]}$Al were experimentally observed using ^{17}O MAS-NMR spectroscopy (Jaworski et al., 2015), an observation corroborated by MD simulations (Okhotnikov et al., 2013).

X-ray absorption spectroscopy (XAS) and NMR were used to determine CNs and infer constraints on the cation clustering by leveraging on MD simulations (Ponader and Brown, 1989; Sen and Stebbins, 1995; Du, 2009; Christie and Tilocca, 2010a; Christie and Tilocca, 2010b; Jaworski et al., 2012; Iftekhar et al., 2012; Pahari et al., 2012; Okhotnikov et al., 2013). The main factors influencing the local RE environment in glasses have been identified (Ponader and Brown, 1989;

Wang et al., 1993; Okhotnikov et al., 2013): as the RE ionic radius increases, the RE-O distances and CNs increase while the sites occupied by RE^{3+} cations become less regular. Lanthanum behaves slightly differently with more regular sites and is considered to be centered in a 'cage' formed by the rings of TO_4 tetrahedra. Due to a large ionic radius ratio ($r_{RE}/r_O > 0.732$) and a strong ionicity of RE-O bonds (Tanabe et al., 1992), CNs for RE^{3+} are larger than for Al^{3+}. Octahedral coordination is the most probable one for the smallest ions (Sc, Lu) and high CNs (7) are observed for large RE cations (La, Y). MD simulations indicate a large distribution of CNs in the range from 4 to 8, with 4-fold and 8-fold coordination being significant only for Sc and La, respectively.

Investigations have established relationships between mechanical properties and structural parameters (Iftekhar et al., 2012; Stevensson and Edén, 2013). The CFS or the network connectivity increase with hardness values. However, ideas have emerged that RE ions impact microhardness indirectly through the formation of $^{[5,6]}Al$. Figure 14 shows an excellent correlation ($R^2 = 0.92$) between Vickers hardness, H_V, and the average Al coordination number for many RE-AS glasses. Therefore, increasing amounts of $^{[5,6]}Al$, originating from the high CFS of RE^{3+} cations, primarily account for the enhanced microhardness. AlO_5 and AlO_6 (and ReO_n) polyhedra are expected to connect different network fragments, yielding a more compact and stiffer network that favors high hardness.

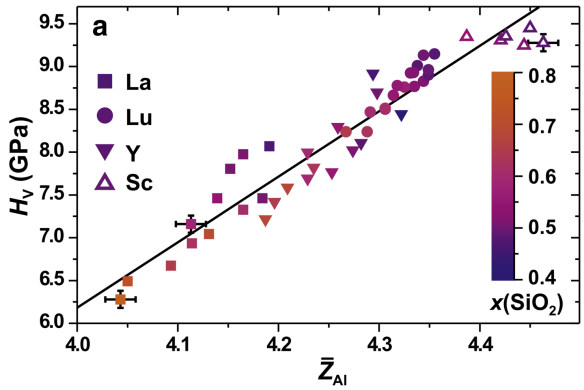

Figure 14. Vickers hardnesss, H_V, as a function of the average Al coordination, $\bar{Z}_{Al}$, for various RE aluminosilicate glasses. The solid line is the best-fit ($H_V = -24 + 7.7\bar{Z}_{Al}$; R2 = 0.92) revealing a strong property/structure correlation. Reprinted with permission from Stevensson and Edén (2013).

Complex aluminosilicate glasses

Chemically complex aluminosilicate glasses are numerous and two aspects have been explored particularly: (i) mixing of different modifiers and (ii) mixing of different framework cations (mainly, B^{3+} or P^{5+}).

When more than one type of non-network forming cation is present in AS glasses, the CFS affects their relative distribution between a modifying or charge balancing position. This type of disorder is mirrored in the preference of NBOs and BOs to be bonded to specific cations and in the formation of $^{[5,6]}$Al. Mixing of non-framework cations has been explored in AS glasses with Ca-Mg (Neuville et al., 2008; Kelsey et al., 2008; Park and Lee, 2012; Smedskjaer et al., 2013; Allu et al., 2018; Ganisetti et al., 2019), Ca-Na (Cormier and Neuville, 2004; Lee and Sung, 2008; Gambuzzi et al., 2014; Sukenaga et al., 2017), Na-K (Le Losq and Neuville, 2013; Le Losq et al., 2017), Na-Mg (Park and Lee, 2018), Ca-Mg-Na (Smedskjaer et al., 2013; Kjeldsen et al., 2013; Park and Lee, 2014; Bechgaard et al., 2017). In presence of alkalis and alkaline-earths, NBOs prefer to have proximity towards M^{2+} cations that preferentially play a role of network modifier, whereas BOs are more associated with M^{+} cations that act as charge balancing cations in, typically, Si-BO-$^{[4]}$Al environments. For Ca/Mg mixing, NBOs tend to have a Mg-rich environment, whereas Ca has a greater propensity to be associated with BOs. The non-randomness in the partitioning of non-framework cations around BOs and NBOs is explained by the CFS: higher CFS ($CFS_{M^{2+}} > CFS_{M^{+}}$ and $CFS_{Mg^{2+}} > CFS_{Ca^{2+}}$) favors proximity of cations to NBOs. However, in a $CaMgSi_2O_6$-$CaAl_2SiO_6$ join, ^{17}O NMR reveals a Ca-NBO-Si peak, suggesting a preferential bonding of NBOs with Ca and/or a potential unmixing of Ca and Mg (Park and Lee, 2012). If the separation between polymerized regions and channels exists (EMRN model, Figure 4), Na^{+} cations will be preferentially localized in the polymerized Al/Si regions close to $^{[4]}$Al to ensure charge compensation, while M^{2+} cations will be in channels associated with NBOs in depolymerized Q_{Si}^{n} species (Gambuzzi et al., 2014; Sukenaga et al., 2017). A major outcome of these studies is an increasing amount of $^{[5]}$Al with CFS. For instance, the fraction of $^{[5]}$Al increases from ~5% to ~20% as Ca is substituted by Mg, emphasizing the lower ability of Mg^{2+} to stabilize $^{[4]}$Al (Neuville et al., 2008; Kelsey et al., 2008).

The degree of Al/B mixing in boroaluminosilicate or boroaluminate glasses plays an essential role in controlling major physical properties such as chemical durability, phase separation, mechanical strength or crystallization behavior (Du et al., 2000; Du and Stebbins, 2005a; Du and Stebbins, 2005b). The presence of B_2O_3 creates complex competition for M^{n+} cations for charge compensation of $(AlO_4)^{-}$ or $(BO_4)^{-}$ tetrahedra (El-Damrawi et al., 1993; Chan et al., 1999; Cormier et al., 2000a; Yamashita et al., 2003; Smedskjaer et al., 2014). M^{n+} cations are firstly consumed to charge stabilize $(AlO_4)^{-}$ units, limiting the formation of higher Al coordination states. The excess M^{n+} cations are used to convert boron from trigonal (BO_3) to tetrahedral (BO_4) configurations. The proportion of BO_4 units, determined by the ratio $N_4 = BO_4 / (BO_4 + BO_3)$, is then lower in boroaluminosilicate glasses compared to borosilicate counterparts. N_4 values increase with decreasing Al_2O_3 content and a maximum value, $N_{4(max)}$, is reached at $R' = ([Na_2O]-[Al_2O_3])/[B_2O_3] = 1$. When $N_4 < N_{4(max)}$ and $M^{n+}/nAl > 1$, NBOs on silicon can also be created but preferential formation of Q_{Si}^{3} over BO_4 is observed depending on the M^{n+} cation type (Yamashita et al., 2003). Figure 15 represents the reactivity

of M_nO with B_2O_3 and SiO_2, showing that formation of Q^3_{Si} species is favored (and formation of BO_4 is disfavored) in the order Mg > Ca > Sr > Ba > Na > K. For compositions with $M^{n+}/nAl < 1$, N_4 values are expected to be equal to zero.

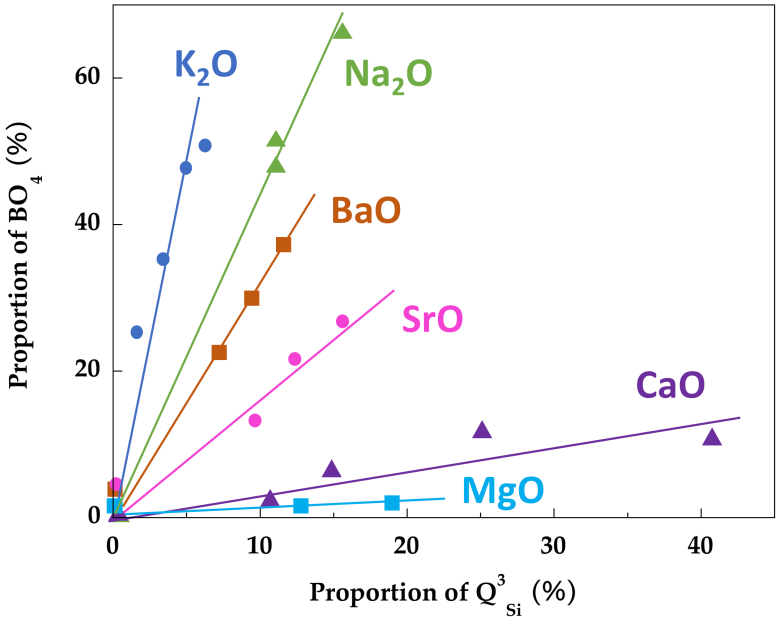

Figure 15. Relation between the fraction of BO_4 and the fraction of Q^3_{Si} in 0.139 $M^{n+}{}_nO$ - 0.673 SiO_2 - (0.188-x) Al_2O_3 - xB_2O_3 (M^{n+}= Na^+, K^+, Mg^{2+}, Ca^{2+}, Sr^{2+} and Ba^{2+}) glasses. Data from Yamashita et al. (2003).

Non-zero population of high-coordinated Al sites are observed in boroaluminosilicate glasses with Na/Al < 1 (Smedskjaer et al., 2014) or in presence of alkaline-earth cations (Bunker, 1991; Baltisberger et al., 1996; Chan et al., 1999; Du and Stebbins, 2005a; Wu and Stebbins, 2009).

Using NMR spectroscopy (Chan et al., 1999; Du and Stebbins, 2005b; Du and Stebbins, 2005a; Angeli, 2001), the various structural linkages between AlO_4, SiO_4, BO_3 or BO_4 can be identified. $^{[4]}$Al-O-$^{[4]}$Al, $^{[4]}$Al-O-$^{[4]}$B and $^{[4]}$B-O-$^{[4]}$B interactions are disfavored (4-4 avoidance) and depend strongly on the composition and the type of cation M^{n+}. In B_2O_3-Al_2O_3(-SiO_2) glasses, strong chemical ordering (4-4 avoidance) is respected with K or Na, whereas a trend toward random mixing is observed with Mg or Ca. High Al and/or low M^{n+} contents favor obedience to 4-4 avoidance. In addition to lowering N_4 values by the formation of $^{[4]}$Al, the addition of Al lowers $N_{4(max)}$ due to the 4-4 avoidance between $^{[4]}$B and $^{[4]}$Al (Du and Stebbins, 2005a). $N_{4(max)}$ values are also higher for higher SiO_2 content since Si atoms limit the possibility of $^{[4]}$B-O-$^{[4]}$Al linkages and allow a higher fraction of $^{[4]}$B. In boroaluminate glasses (Chan et al., 1999; Wang and Stebbins, 2004; Du and Stebbins, 2005b), $^{[n]}$Al units interact with the dominant BO_3 sites without forming Al enriched regions or Al-O-Al linkages. $^{[4]}$Al-O-$^{[3]}$B linkages

are more probable than $^{[4]}$Al-O-$^{[4]}$B one and they are energetically more stable than $^{[4]}$B-O-$^{[4]}$B and $^{[4]}$Al-O-$^{[4]}$Al ones. $^{[4]}$B interacts preferentially with $^{[5,6]}$Al rather than $^{[4]}$Al, suggesting that $^{[5,6]}$Al species are stabilizing $^{[4]}$B.

REFERENCES

Aasland, S., McMillan, P.F., 1994. Density-driven liquid-liquid phase separation in the system Al_2O_3-Y_2O_3. *Nature* **369**, 633-636. https://doi.org/10.1038/369633a0

Agnello, G., Youngman, R., Lamberson, L., Smith, N., LaCourse, W., Cormack, A.N., 2019. Bulk structures of silica-rich calcium aluminosilicate (CAS) glasses along the molar CaO/Al_2O_3 = 1 join via molecular dynamics (MD) simulation. *Journal of Non-Crystalline Solids* **519**, 119450. https://doi.org/10.1016/j.jnoncrysol.2019.05.026

Akola, J., Kohara, S., Ohara, K., Fujiwara, A., Watanabe, Y., Masuno, A., Usuki, T., Kubo, T., Nakahira, A., Nitta, K., Uruga, T., Weber, J.K.R., Benmore, C.J., 2013. Network topology for the formation of solvated electrons in binary CaO-Al_2O_3 composition glasses. *Proceedings of the National Academy of Sciences* **110**, 10129-10134. https://doi.org/10.1073/pnas.1300908110

Alahrache, S., 2011. Vitrocéramiques transparentes d'aluminates : mécanismes de cristallisation et étude structurale. Université d'Orléans, Orléans.

Allu, A.R., Gaddam, A., Ganisetti, S., Balaji, S., Siegel, R., Mather, G.C., Fabian, M., Pascual, M.J., Ditaranto, N., Milius, W., Senker, J., Agarkov, D.A., Kharton, Vladislav.V., Ferreira, J.M.F., 2018. Structure and Crystallization of Alkaline-Earth Aluminosilicate Glasses: Prevention of the Alumina-Avoidance Principle. *The Journal of Physical Chemistry B* **122**, 4737-4747. https://doi.org/10.1021/acs.jpcb.8b01811

Allwardt, J.R., Lee, S.K., Stebbins, J.F., 2003. Bonding preferences of non-bridging O atoms: evidence from ^{17}O MAS and 3QMAS NMR on calcium aluminate and low-silica Ca-aluminosilicate glasses. *American Mineralogist* **88**, 949-954.

Allwardt, J.R., Poe, B.T., Stebbins, J.F., 2005a. The effect of fictive temperature on Al coordination in high pressure (10 GPa) sodium aluminosilicate glasses. *American Mineralogist* **90**, 1453-1457.

Allwardt, J.R., Stebbins, J.F., Schmidt, B.C., Frost, D.J., Withers, A.C., Hirschmann, M.M., 2005b. Aluminum coordination and the densification of high-pressure aluminosilicate glasses. *American Mineralogist* **90**, 1218-1222.

Allwardt, J.R., Stebbins, J.F.,. terasaki, H.,. Du, L.S.,. Frost, D.J.,. Withers, A.C.,. Hirschmann, M.M.,. Suzuki, A.,. Ohtani, E., 2007. Effect of structural transition on properties of high-pressure silicate melts: ^{27}Al NMR, glass densities, and melt viscosities. *American Mineralogist* **92**, 1093-1104.

Ando, M.F., Benzine, O., Pan, Z., Garden, J.-L., Wondraczek, K., Grimm, S., Schuster, K., Wondraczek, L., 2018. Boson peak, heterogeneity and intermediate-range order in binary SiO_2-Al_2O_3 glasses. *Scientific Reports* **8**, 5394. https://doi.org/10.1038/s41598-018-23574-1

Angeli, F., Charpentier, T.,. Gin, S.,. Petit, J.C., 2001. ^{17}O 3Q-MAS NMR characterization of a sodium aluminoborosilicate glass and its alteration gel. *Chemical Physics Letters* **341**, 23-28.

Atila, A., Ghardi, E.M., Hasnaoui, A., Ouaskit, S., 2019. Alumina effect on the structure and properties of calcium aluminosilicate in the percalcic region: A molecular dynamics investigation. *Journal of Non-Crystalline Solids* **525**, 119470. https://doi.org/10.1016/j.jnoncrysol.2019.119470

Baltisberger, J.H., Xu, Z., Stebbins, J.F., Wang, S.H., Pines, A., 1996. Triple-Quantum Two-Dimensional ^{27}Al Magic-Angle Spinning Nuclear Magnetic Resonance Spectroscopic Study of Aluminosilicate and Aluminate Crystals and Glasses. *Journal of the American Chemical Socety* **118**, 7209-7214. https://doi.org/10.1021/ja9606586

Barbieri, L., Corradi, A.B., Lancellotti, I., Leonelli, C., Montorsi, M., 2004. Experimental and computer simulation study of glasses belonging to diopside-anorthite system. *Journal of Non-Crystalline Solids* **345-346**, 724-729. https://doi.org/10.1016/j.jnoncrysol.2004.08.190

Bardez, I., Caurant, D., Loiseau, P., Baffier, N., Dussossoy, J.L., Gervais, C., Ribot, F., Neuville, D.R., 2005. Structural characterisation of rare earth rich glasses for nuclear waste immobilisation. *Physics and Chemistry of Glasses* **46**, 320-329.

Barnes, A.C., Skinner, L.B.,. Salmon, P.S.,. Bytchkov, A.,. Pozdnyakova, I.,. Farler, T.O.,. Fischer, H.E., 2009. Liquid-Liquid Phase Transition in Supercooled Yttria-Alumina. *Physical Review Letters* **103**, 225702.

Bechgaard, T.K., Scannell, G., Huang, L., Youngman, R.E., Mauro, J.C., Smedskjaer, M.M., 2017. Structure of MgO/CaO sodium aluminosilicate glasses: Raman spectroscopy study. *Journal of Non-Crystalline Solids*

470, 145-151. https://doi.org/10.1016/j.jnoncrysol.2017.05.014
Benmore, C.J., Weber, J.K.R., Sampath, S., Siewenie, J., Urquidi, J., Tangeman, J.A., 2003. A neutron and x-ray diffraction study of calcium aluminate glasses. *Journal of Physics: Condensed Matter* **15**, S2413-S2423. https://doi.org/10.1088/0953-8984/15/31/316
Benoit, M., Profeta, M., Mauri, F., Pickard, C.J., Tuckerman, M.E., 2005. First-Principles Calculation of the ^{17}O NMR Parameters of a Calcium Aluminosilicate Glass. *The Journal of Physical Chemistry B* **109**, 6052-6060. https://doi.org/10.1021/jp0492570
Bista, S., Stebbins, J.F., Hankins, W.B., Sisson, T.W., 2015. Aluminosilicate melts and glasses at 1 to 3 GPa: Temperature and pressure effects on recovered structural and density changes. *American Mineralogist* **100**, 2298-2307. https://doi.org/10.2138/am-2015-5258
Bouhadja, M., Jakse, N., Pasturel, A., 2014. Striking role of non-bridging oxygen on glass transition temperature of calcium aluminosilicate glass-formers. *Journal of Chemical Physics* **140**, 234507. https://doi.org/10.1063/1.4882283
Brawer, S.A., White, W.B., 1977. Raman spectroscopic investigation of the structure of silicate glasses (II. Soda-alkaline earth-alumina ternary and quaternary glasses. *Journal of Non-Crystalline Solids* **23**, 261-278.
Brower, K.L., 1979. Electron paramagnetic resonance of Al E 1 ′ centers in vitreous silica. *Physical Review B* **20**, 1799-1811. https://doi.org/10.1103/PhysRevB.20.1799
Brower, K.L., 1978. Structural and Trapping Characteristics of a New Al Defect in Vitreous Silica. *Physical Review Letters* **41**, 879-881. https://doi.org/10.1103/PhysRevLett.41.879
Bunker, B.C., Kirkpatrick, R.J., Brow, R.K., Turner, G.L., Nelson, C., 1991. Local structure of alkaline-earth boroaluminate crystals and glasses: II, ^{11}B and ^{27}Al MAS NMR spectroscopy of alkaline-earth boroaluminate glasses. *Journal of the American Ceramic Society* **74**, 1430-1438.
Chan, J.C.C., Bertmer, M., Eckert, H., 1999. Site Connectivities in Amorphous Materials Studied by Double-Resonance NMR of Quadrupolar Nuclei: High-Resolution $^{11}B \leftrightarrow {}^{27}Al$ Spectroscopy of Aluminoborate Glasses. *Journal of the American Chemical Society* **121**, 5238-5248. https://doi.org/10.1021/ja983385i
Charpentier, T., Okhotnikov, K., Novikov, A.N., Hennet, L., Fischer, H.E., Neuville, D.R., Florian, P., 2018. Structure of Strontium Aluminosilicate Glasses from Molecular Dynamics Simulation, Neutron Diffraction, and Nuclear Magnetic Resonance Studies. *The Journal of Physical Chemistry B* **122**, 9567-9583. https://doi.org/10.1021/acs.jpcb.8b05721
Christie, J.K., Tilocca, A., 2010a. Short-Range Structure of Yttrium Alumino-Silicate Glass for Cancer Radiotherapy: Car-Parrinello Molecular Dynamics Simulations. *Advanced Engineering Materials***12**, B326-B330. https://doi.org/10.1002/adem.200980081
Christie, J.K., Tilocca, A., 2010b. Aluminosilicate Glasses As Yttrium Vectors for in situ Radiotherapy: Understanding Composition-Durability Effects through Molecular Dynamics Simulations. *Chemistry of Materials***22**, 3725-3734. https://doi.org/10.1021/cm100847p
Clayden, N.J., Esposito, S., Aronne, A., Pernice, P., 1999. Solid state ^{27}Al NMR and FTIR study of lanthanum aluminosilicate glasses. *Journal of Non-Crystalline Solids* **258**, 11-19. https://doi.org/10.1016/S0022-3093(99)00555-4
Cormier, L., Calas, G.,. Creux, S.,. Gaskell, P.H.,. Bouchet-Fabre, B.,. Hannon, A.C., 1999. Environment around strontium in silicate and aluminosilicate glasses. *Physical Review B* **59**, 13517-13520.
Cormier, L., Delbes, L., Baptiste, B., Montouillout, V., 2021. Vitrification, crystallization behavior and structure of zinc aluminosilicate glasses. *Journal of Non-Crystalline Solids*
Cormier, L., Galoisy, L.,. Delaye, J.M.,. Ghaleb, D.,. Calas, G., 2001. Short- and medium-range structural order around cations in glasses: a multidisciplinary approach. *CR Acad Sci Sér. IV* **2**, 249-262.
Cormier, L., Gaskell, P.H.,. Calas, G.,. Zhao, J.,. Soper, A.K., 1998. The environment around Li in the $LiAlSiO_4$ ionic conductor glass: a neutron scattering and reverse Monte Carlo study. *Physical Review B* 57, R8067-R8070.
Cormier, L., Ghaleb, D., Delaye, J.M., Calas, G., 2000a. Competition for charge compensation in borosilicate glasses: Wide-angle x-ray scattering and molecular dynamics calculations. *Physical Review B* **61**, 14495-14999.
Cormier, L., Ghaleb, D., Neuville, D.R., Delaye, J.-M., Calas, G., 2003. Chemical dependence of network topology of calcium aluminosilicate glasses: a computer simulation study. *Journal of Non-Crystalline Solids* **332**, 255-270. https://doi.org/10.1016/j.jnoncrysol.2003.09.012
Cormier, L., Neuville, D.R., 2004. Ca and Na environments in Na_2O-CaO-Al_2O_3-SiO_2 glasses: influence of cation mixing and cation-network interactions. *Chemical Geology* **213**, 103-113. https://doi.org/10.1016/j.chemgeo.2004.08.049
Cormier, L., Neuville, D.R., Calas, G., 2005. Relationship Between Structure and Glass Transition Temperature in Low-silica Calcium Aluminosilicate Glasses: the Origin of the Anomaly at Low Silica Content: Structure and Glass Transition Temperature Relationship. *Journal of the American Ceramic Society* **88**, 2292-2299. https://doi.org/10.1111/j.1551-2916.2005.00428.x

Cormier, L., Neuville, D.R., Calas, G., 2000b. Structure and properties of low-silica calcium aluminosilicate glasses. *Journal of Non-Crystalline Solids* **274**, 110-114. https://doi.org/10.1016/S0022-3093(00)00209-X

Cristiglio, V., Hennet, L., Cuello, G.J., Johnson, M.R., Fernández-Martínez, A., Fischer, H.E., Pozdnyakova, I., Zanghi, D., Brassamin, S., Brun, J.-F., Price, D.L., 2007. Ab-initio molecular dynamics simulations of the structure of liquid aluminates. *Journal of Non-Crystalline Solids* **353**, 1789-1792. https://doi.org/10.1016/j.jnoncrysol.2007.01.075

Day, D.E., Rindone, G.E., 1962. Properties of Soda Aluminosilicate Glasses: I, Refractive Index, Density, Molar Refractivity, and Infrared Absorption Spectra. *Journal of the American Ceramic Society* **45**, 489-496. https://doi.org/10.1111/j.1151-2916.1962.tb11040.x

Douy, A., Gervais, M., 2000. Crystallization of Amorphous Precursors in the CalciaAlumina System: A Differential Scanning Calorimetry Study. *Journal of the American Ceramic Society* **83**, 70-76. https://doi.org/10.1111/j.1151-2916.2000.tb01150.x

Drewitt, J.W.E., Jahn, S., Cristiglio, V., Bytchkov, A., Leydier, M., Brassamin, S., Fischer, H.E., Hennet, L., 2011. The structure of liquid calcium aluminates as investigated using neutron and high energy x-ray diffraction in combination with molecular dynamics simulation methods. *Journal of Physics: Condensed Matter* **23**, 155101.

Du, J., 2009. Molecular Dynamics Simulations of the Structure and Properties of Low Silica Yttrium Aluminosilicate Glasses. *Journal of the American Ceramic Society* **92**, 87-95. https://doi.org/10.1111/j.1551-2916.2008.02853.x

Du, J., Benmore, C.J., Corrales, R., Hart, R.T., Weber, J.K.R., 2009. A molecular dynamics simulation interpretation of neutron and x-ray diffraction measurements on single phase Y_2O_3-Al_2O_3 glasses. *Journal of Physics: Condensed Matter* **21**, 205102. https://doi.org/10.1088/0953-8984/21/20/205102

Du, J., René Corrales, L., 2007. Understanding lanthanum aluminate glass structure by correlating molecular dynamics simulation results with neutron and X-ray scattering data. *Journal of Non-Crystalline Solids* **353**, 210-214. https://doi.org/10.1016/j.jnoncrysol.2006.06.025

Du, L.-S., Stebbins, J.F., 2005a. Network connectivity in aluminoborosilicate glasses: A high-resolution ^{11}B, ^{27}Al and ^{17}O NMR study. *Journal of Non-Crystalline Solids* **351**, 3508-3520. https://doi.org/10.1016/j.jnoncrysol.2005.08.033

Du, L.-S., Stebbins, J.F., 2005b. Site connectivities in sodium aluminoborate glasses: multinuclear and multiple quantum NMR results. *Solid State Nuclear Magnetic Resonance* **27**, 37-49. https://doi.org/10.1016/j.ssnmr.2004.08.003

Du, W.-F., Kuraoka, K., Akai, T., Yazawa, T., 2000. Study of Al_2O_3 effect on structural change and phase separation in Na2O-B2O3-SiO2 glass by NMR. *Journal of Materials Science* **35**, 4865-4871. https://doi.org/10.1023/A:1004853603298

Dubinsky, E.V., 2006. Quench rate and temperature effects on framework ordering in aluminosilicate melts. *American Mineralogist* **91**, 753-761. https://doi.org/10.2138/am.2006.2039

Edén, M., 2015. ^{27}Al NMR Studies of Aluminosilicate Glasses, in: *Annual Reports on NMR Spectroscopy*. Elsevier, pp. 237-331. https://doi.org/10.1016/bs.arnmr.2015.04.004

Edwards, P.P., 2011. Electrons in Cement. *Science* **333**, 49-50. https://doi.org/10.1126/science.1207837

El-Damrawi, G., Müller-Warmuth, W., Doweidar, H., Gohar, I.A., 1993. ^{11}B, ^{29}Si and ^{27}Al nuclear magnetic resonance studies of Na_2O-Al_2O_3-B_2O_3-SiO_2 glasses. *Physics and Chemistry of Glasses* **34**, 52-57.

Engelhardt, G., 1989. Multinuclear solid-state NMR in silicate and zeolite chemistry. *TrAC Trends Anal. Chem.* **8**, 343-347. https://doi.org/10.1016/0165-9936(89)87043-8

Engelhardt, G., Nofz, M., Forkel, K., Wihsmann, F.G., Mägi, M., Samoson, A., Lippmaa, E., 1985. Structural studies of calcium aluminosilicate glasses by high resolution solid state ^{29}Si and ^{27}Al magic angle spinning nuclear magnetic resonance. *Physics and Chemistry of Glasses* **26**, 157-165.

Farnan, I., Stebbins, J.F., 1994. The nature of the glass transition in a silica-rich oxide melt. *Science* **265**, 1206-1208.

Florian, P., Gervais, M., Douy, A., Massiot, D., Coutures, J.-P., 2001. A Multi-nuclear Multiple-Field Nuclear Magnetic Resonance Study of the Y_2O_3-Al_2O_3 Phase Diagram. *The Journal of Physical Chemistry B* **105**, 379-391. https://doi.org/10.1021/jp0008851

Florian, P., Sadiki, N.,. Massiot, D.,. Coutures, J.P., 2007. 27Al NMR study of the structure of lanthanum- and yttrium-based aluminosilicate glasses and melts. *The Journal of Physical Chemistry B* **111**, 9747-9757.

Gambuzzi, E., Pedone, A., Menziani, M.C., Angeli, F., Caurant, D., Charpentier, T., 2014. Probing silicon and aluminium chemical environments in silicate and aluminosilicate glasses by solid state NMR spectroscopy and accurate first-principles calculations. *Geochimica et Cosmochimica Acta* **125**, 170-185. https://doi.org/10.1016/j.gca.2013.10.025

Ganisetti, S., Gaddam, A., Kumar, R., Balaji, S., Mather, G.C., Pascual, M.J., Fabian, M., Siegel, R., Senker, J., Kharton, V.V., Guénolé, J., Krishnan, N.M.A., Ferreira, J.M.F., Allu, A.R., 2019. Elucidating the formation of Al-NBO bonds, Al-O-Al linkages and clusters in alkaline-earth aluminosilicate glasses based on

molecular dynamics simulations. *Physical Chemistry Chemical Physics* **21**, 23966-23977. https://doi.org/10.1039/C9CP04332B

Greaves, G.N., Ngai, K.L., 1995a. Reconciling ionic-transport properties with atomic structure in oxide glasses. *Physical Review B* **52**, 6358-6380. https://doi.org/10.1103/PhysRevB.52.6358

Greaves, G.N., Ngai, K.L., 1995b. Relating the atomic structure of alumino-silicate glasses to their ionic transport properties. *Journal of Non-Crystalline Solids* **192-193**, 405-410. https://doi.org/10.1016/0022-3093(95)00382-7

Greaves, G.N., Wilding, M.C.,. Fearn, S.,. Kargl, F.,. Hennet, L.,. Bras, W.,. Majérus, O.,. Martin, C.M., 2009. Liquid-liquid transitions, crystallization and long range fluctuations in supercooled yttrium oxide-aluminium oxide melts. *Journal of Non-Crystalline Solids* **355**, 715-721.

Greaves, G.N., Wilding, M.C.,. Fearn, S.,. Langstaff, D.,. Kargl, F.,. Cox, S.,. Vu Van, Q.,. Majérus, O.,. Benmore, C.J.,. Weber, R.,. Martin C.M.,. Hennet, L., 2008. Detection of first-order liquid/liquid phase trasitions in yttrium oxide-aluminum oxide melts. *Science* **322**, 566-570.

Guignard, M., Cormier, L., 2008. Environments of Mg and Al in MgO-Al_2O_3-SiO_2 glasses: A study coupling neutron and X-ray diffraction and Reverse Monte Carlo modeling. *Chemical Geology* **256**, 111-118. https://doi.org/10.1016/j.chemgeo.2008.06.008

Hafner, H.C., Kreidl, N.J., Weidel, R.A., 1958. Optical and Physical Properties of Some Calcium Aluminate Glasses. *Journal of the American Ceramic Society* **41**, 315-323. https://doi.org/10.1111/j.1151-2916.1958.tb12923.x

Hannon, A.C., Parker, J.M., 2000. The structure of aluminate glasses by neutron diffraction. *Journal of Non-Crystalline Solids* **274**, 102-109. https://doi.org/10.1016/S0022-3093(00)00208-8

Hiet, J., Deschamp, M.,. Pellerin, N.,. Fayon, F.,. Massiot, D., 2009. Probing chemical disorder in glasses using silicon-29 NMR spectral editing. *Physical Chemistry Chemical Physics* **11**, 6935-6940.

Higby, P.L., Ginther, R.J.,. Aggarwal, I.D.,. Friebele, E.J., 1990. Glass formation and thermal properties of low-silica calcium aluminosilicate glasses. *Journal of Non-Crystalline Solids* **126**, 209-215.

Himmel, B., Weigelt, J.,. Gerber, T.,. Nofz, M., 1991. Structure of calcium aluminosilicate glasses: wide-angle X-ray scattering and computer simulation. *Journal of Non-Crystalline Solids* **136**, 27-36.

Hoang, V.V., 2007. Composition dependence of static and dynamic heterogeneities in simulated liquid aluminum silicates. *Physical Review B* **75**, 174202. https://doi.org/10.1103/PhysRevB.75.174202

Hosono, H., Abe, Y., 1987. An Oxygen-Effervescent Aluminate Glass. *Journal of the American Ceramic Society* **70**, C-38-C-39. https://doi.org/10.1111/j.1151-2916.1987.tb04958.x

Hosono, H., Yamazaki, K., Abe, Y., 1985. Dopant-Free Ultraviolet-Sensitive Calcium Aluminate Glasses. *Journal of the American Ceramic Society* **68**, C-304-C-305. https://doi.org/10.1111/j.1151-2916.1985.tb16151.x

Hwa, L.-G., 1998. Rayleigh-Brillouin Scattering in Calcium Aluminosilicate Glasses. *Journal of Raman Spectroscopy* **29**, 269-272.

Hyatt, M.J., Day, D.E., 1987. Glass Properties in the Yttria-Alumina-Silica System. *Journal of the American Ceramic Society* **70**, C-283-C-287. https://doi.org/10.1111/j.1151-2916.1987.tb04901.x

Iftekhar, S., Grins, J., Gunawidjaja, P.N., Edén, M., 2011. Glass Formation and Structure-Property-Composition Relations of the RE_2O_3-Al_2O_3-SiO_2 (RE=La, Y, Lu, Sc) Systems: Rare-Earth Aluminosilicate Glasses. *Journal of the American Ceramic Society* **94**, 2429-2435. https://doi.org/10.1111/j.1551-2916.2011.04548.x

Iftekhar, S., Leonova, E., Edén, M., 2009. Structural characterization of lanthanum aluminosilicate glasses by ^{29}Si solid-state NMR. *Journal of Non-Crystalline Solids* **355**, 2165-2174. https://doi.org/10.1016/j.jnoncrysol.2009.06.031

Iftekhar, S., Pahari, B., Okhotnikov, K., Jaworski, A., Stevensson, B., Grins, J., Edén, M., 2012. Properties and Structures of RE_2O_3-Al_2O_3-SiO_2 (RE = Y, Lu) Glasses Probed by Molecular Dynamics Simulations and Solid-State NMR: The Roles of Aluminum and Rare-Earth Ions for Dictating the Microhardness. *The Journal of Physical Chemistry C* **116**, 18394-18406. https://doi.org/10.1021/jp302672b

Inaba, S., Todaka, S., Ohta, Y., Morinaga, K., 2000. Equation for Estimating the Young's Modulus, Shear Modulus and Vickers Hardness of Aluminosilicate Glasses. *Journal of The Japan Institute of Metals***64**, 177-183. https://doi.org/10.2320/jinstmet1952.64.3_177

Iuga, D., Morais, C., Gan, Z., Neuville, D.R., Cormier, L., Massiot, D., 2005. NMR Heteronuclear Correlation between Quadrupolar Nuclei in Solids. *Journal of the American Chemical Society* **127**, 11540-11541. https://doi.org/10.1021/ja052452n

Jakse, N., Bouhadja, M., Kozaily, J., Drewitt, J.W.E., Hennet, L., Neuville, D.R., Fischer, H.E., Cristiglio, V., Pasturel, A., 2012. Interplay between non-bridging oxygen, triclusters, and fivefold Al coordination in low silica content calcium aluminosilicate melts. *Applied Physics Letters* **101**, 201903. https://doi.org/10.1063/1.4766920

Jaworski, A., Stevensson, B., Edén, M., 2015. Direct ^{17}O NMR experimental evidence for Al-NBO bonds in Si-

rich and highly polymerized aluminosilicate glasses. *Physical Chemistry Chemical Physics* **17**, 18269-18272. https://doi.org/10.1039/C5CP02985F

Jaworski, A., Stevensson, B., Pahari, B., Okhotnikov, K., Edén, M., 2012. Local structures and Al/Si ordering in lanthanum aluminosilicate glasses explored by advanced ^{27}Al NMR experiments and molecular dynamics simulations. *Physical Chemistry Chemical Physics* **14**, 15866. https://doi.org/10.1039/c2cp42858j

Johnson, J., Weber, R., Grimsditch, M., 2005. Thermal and mechanical properties of rare earth aluminate and low-silica aluminosilicate optical glasses. *Journal of Non-Crystalline Solids* **351**, 650-655. https://doi.org/10.1016/j.jnoncrysol.2005.01.065

Kanehashi, K., Stebbins, J.F., 2007. In situ high temperature ^{27}Al NMR study of structure and dynamics in a calcium aluminosilicate glass and melt. *Journal of Non-Crystalline Solids* **353**, 4001-4010. https://doi.org/10.1016/j.jnoncrysol.2007.06.030

Kang, E.-T., Lee, S.-J., Hannon, A.C., 2006. Molecular dynamics simulations of calcium aluminate glasses. *Journal of Non-Crystalline Solids* **352**, 725-736. https://doi.org/10.1016/j.jnoncrysol.2006.02.013

Kelsey, K.E., Allwardt, J.R., Stebbins, J.F., 2008. Ca-Mg mixing in aluminosilicate glasses: An investigation using ^{17}O MAS and 3QMAS and ^{27}Al MAS NMR. *Journal of Non-Crystalline Solids* **354**, 4644-4653. https://doi.org/10.1016/j.jnoncrysol.2008.05.049

Kelsey, K.E., Stebbins, J.F., Singer, D.M., Brown, G.E., Mosenfelder, J.L., Asimow, P.D., 2009. Cation field strength effects on high pressure aluminosilicate glass structure: Multinuclear NMR and La XAFS results. *Geochimica et Cosmochimica Acta* **73**, 3914-3933. https://doi.org/10.1016/j.gca.2009.03.040

Kidari, A., Dussossoy, J.L., Brackx, E., Caurant, D., Magnin, M., Bardez-Giboire, I., 2012. Lanthanum and neodymium solubility in simplified SiO_2-B_2O_3-Na_2O-Al_2O_3-CaO high level waste glass. *Journal of the American Ceramic Society* **95**, 2537-2544. https://doi.org/10.1111/j.1551-2916.2012.05273.x

Kim, S.W., Shimoyama, T., Hosono, H., 2011. Solvated Electrons in High-Temperature Melts and Glasses of the Room-Temperature Stable Electride $[Ca_{24}Al_{28}O_{64}]^{4+}$*4e-. *Science* **333**, 71-74. https://doi.org/10.1126/science.1204394

Kjeldsen, J., Smedskjaer, M.M., Mauro, J.C., Youngman, R.E., Huang, L., Yue, Y., 2013. Mixed alkaline earth effect in sodium aluminosilicate glasses. *Journal of Non-Crystalline Solids* **369**, 61-68. https://doi.org/10.1016/j.jnoncrysol.2013.03.015

Kubicki, J.D., Toplis, M.J., 2002. Molecular orbital calculations on aluminosilicate tricluster molecules: implications for the structure of aluminosilicate glasses. *American Mineralogist* **87**, 668-678.

Lacy, E.D., 1963. Aluminium in glasses and in melts. *Physics and Chemistry of Glasses* 4, 234-238.

Lægsgaard, J., 2002. Theory of Al_2O_3 incorporation in SiO_2. *Physical Review B* **65**, 174104. https://doi.org/10.1103/PhysRevB.65.174104

Lamberson, L.A., 2016. Influence of atomic structure on plastic deformation in tectosilicate calcium-aluminosilicate, magnesium-aluminosilicate, and calcium-galliosilicate glasses. PhD Thesis. Cornell University, USA.

Landron, C., Cote, B., Massiot, D., Coutures, J.P., Flank, A.M., Flank, A.M., 1992. Aluminium XAS and NMR Spectroscopic Studies of Calcium Aluminosilicate Glasses. *Physica Status Solidi B* **171**, 9-20. https://doi.org/10.1002/pssb.2221710102

Le Losq, C., Neuville, D.R., 2013. Effect of the Na/K mixing on the structure and the rheology of tectosilicate silica-rich melts. *Chemical Geology* **346**, 57-71. https://doi.org/10.1016/j.chemgeo.2012.09.009

Le Losq, C., Neuville, D.R., Chen, W., Florian, P., Massiot, D., Zhou, Z., Greaves, G.N., 2017. Percolation channels: a universal idea to describe the atomic structure and dynamics of glasses and melts. *Scientific Reports* **7**, 16490. https://doi.org/10.1038/s41598-017-16741-3

Le Losq, C., Neuville, D.R., Florian, P., Henderson, G.S., Massiot, D., 2014. The role of Al^{3+} on rheology and structural changes in sodium silicate and aluminosilicate glasses and melts. *Geochimica et Cosmochimica Acta* **126**, 495-517. https://doi.org/10.1016/j.gca.2013.11.010

Lee, S.K., 2010. Effect of pressure on structure of oxide glasses at high pressure: Insights from solid-state NMR of quadrupolar nuclides. *Solid State Nuclear Magnetic Resonance* **38**, 45-57. https://doi.org/10.1016/j.ssnmr.2010.10.002

Lee, S.K., 2004. Structure of silicate glasses and melts at high pressure: quantum chemical calculations and solid-state NMR. *The Journal of Physical Chemistry B* **108**, 5889-5900.

Lee, S.K., Cody, G.D., Fey, Y., Mysen, B.O., 2004. Nature of polymerization and properties of silicate melts and glasses at high pressure. *Geochimica et Cosmochimica Acta* **68**, 4189-4200.

Lee, S.K., Cody, G.D., Mysen, B.O., 2005. Structure and extent of disorder in quaternary (Ca-Mg and Ca-Na) aluminosilicate glasses and melts. *American Mineralogist* **90**, 1393-1401.

Lee, S.K., Kim, H.-I., Kim, E.J., Mun, K.Y., Ryu, S., 2016. Extent of Disorder in Magnesium Aluminosilicate Glasses: Insights from ^{27}Al and ^{17}O NMR. *The Journal of Physical Chemistry C* **120**, 737-749. https://doi.org/10.1021/acs.jpcc.5b10799

Lee, S.K., Stebbins, J.F., 2009. Effects of the degree of polymerization on the structure of sodium silicate and

aluminosilicate glasses and melts: An ^{17}O NMR study. *Geochimica et Cosmochimica Acta* **73**, 1109-1119. https://doi.org/10.1016/j.gca.2008.10.040
Lee, S.K., Stebbins, J.F., 2006. Disorder and the extent of polymerization in calcium silicate and aluminosilicate glasses: O-17 NMR results and quantum chemical molecular orbital calculations. *Geochimica et Cosmochimica Acta* **70**, 4275-4286.
Lee, S.K., Stebbins, J.F., 2002. Extent of intermixing among framework units in silicate glasses and melts. *Geochimica et Cosmochimica Acta* **66**, 303-309.
Lee, S.K., Stebbins, J.F., 2000a. Al-O-Al and Si-O-Si sites in framework aluminosilicate glasses with Si/Al=1: quantification of framework disorder. *Journal of Non-Crystalline Solids* **270**, 260-264. https://doi.org/10.1016/S0022-3093(00)00089-2
Lee, S.K., Stebbins, J.F., 2000b. The structure of aluminosilicate glasses: high-resolution ^{17}O and ^{27}Al MAS and 3QMAS NMR study. *The Journal of Physical Chemistry B* **104**, 4091-4100.
Lee, S.K., Stebbins, J.F., 1999. The degree of aluminum avoidance in aluminosilicate glasses. *American Mineralogist* **84**, 937-945.
Lee, S.K., Sung, S., 2008. The effect of network-modifying cations on the structure and disorder in peralkaline Ca-Na aluminosilicate glasses: O-17 3QMAS NMR study. *Chemical Geology* **256**, 326-333. https://doi.org/10.1016/j.chemgeo.2008.07.019
Li, W., Garofalini, S.H., 2004. Molecular Dynamics simulation of lithium diffusion in Li_2O-Al_2O_3-SiO_2 glasses. *Solid State Ionics* **166**, 365-373.
Licheron, M., Montouillout, V., Millot, F., Neuville, D.R., 2011. Raman and ^{27}Al NMR structure investigations of aluminate glasses: $(1-x)Al_2O_3-x$ MO, with M=Ca, Sr, Ba and $0.5<x<0.75$. *Journal of Non-Crystalline Solids* **357**, 2796-2801. https://doi.org/10.1016/j.jnoncrysol.2011.03.001
Lin, S.-L., Hwang, C.-S., Lee, J.-F., 1996. Characterization of CeO_2-Al_2O_3-SiO_2 glasses by infrared and x-ray absorption near edge structure spectroscopies. *Journal of Materials Research* **11**, 2641-2650. https://doi.org/10.1557/JMR.1996.0332
Lines, M.E., MacChesney, J.B., Lyons, K.B., Bruce, A.J., Miller, A.E., Nassau, K., 1989. Calcium aluminate glasses as pontential ultralow-loss optical materials at 1.5-1.9 μm. *Journal of Non-Crystalline Solids* **107**, 251-260. https://doi.org/10.1016/0022-3093(89)90470-5
Loewenstein, W., 1954. The distribution of aluminum in the tetrahedra of silicates and aluminates. *American Mineralogist* **39**, 92-96.
Loiseau, P., Caurant, D., 2010. Glass-ceramic nuclear waste forms obtained by crystallization of SiO_2-Al_2O_3-CaO-ZrO_2-TiO_2 glasses containing lanthanides (Ce, Nd, Eu, Gd, Yb) and actinides (Th): Study of the crystallization from the surface. *Journal of Nuclear Materials* **402**, 38-54. https://doi.org/10.1016/j.jnucmat.2010.04.021
Luo, J., Vargheese, K.D., Tandia, A., Harris, J.T., Mauro, J.C., 2016. Structural origin of intrinsic ductility in binary aluminosilicate glasses. *Journal of Non-Crystalline Solids* **452**, 297-306. https://doi.org/10.1016/j.jnoncrysol.2016.09.010
Macdowell, J.F., Beall, G.H., 1969. Immiscibility and Crystallization in Al_2O_3-SiO_2 Glasses. *Journal of the American Ceramic Society* **52**, 17-25. https://doi.org/10.1111/j.1151-2916.1969.tb12653.x
Makishima, A., Kobayashi, M., Shimohira, T., Nagata, T., 1982. Formation of Aluminosilicate Glasses Containing Rare-Earth Oxides. *Journal of the American Ceramic Society* **65**, C-210-C-211. https://doi.org/10.1111/j.1151-2916.1982.tb09954.x
Makishima, A., Tamura, Y., Sakaino, T., 1978. Elastic Moduli and Refractive Indices of Aluminosilicate Glasses Containing Y_2O_3, La_2O_3, and TiO_2. *Journal of the American Ceramic Society* **61**, 247-249. https://doi.org/10.1111/j.1151-2916.1978.tb09291.x
McKeown, D.A., Galeener, F.L., Brown, G.E.Jr., 1984. Raman studies of Al coordination in silica-rich sodium aluminosilicate glasses and some related minerals. *Journal of Non-Crystalline Solids* **68**, 361-378.
McKeown, D.A., Waychunas, G.A.,. Brown, Jr.,.G.E., 1985. EXAFS study of the coordination environment of aluminium in a series of silica-rich glasses and selected minerals within the Na_2O-Al_2O_3-SiO_2 system. *Journal of Non-Crystalline Solids* **74**, 349-371.
McMillan, P.F., Kirkpatrick, R.J., 1992. Al coordination in magnesium aluminosilicate glasses. *American Mineralogist* **77**, 898-900.
McMillan, P.F., Petuskey, W.T., Coté, B., Massiot, D., Landron, C., Coutures, J.P., 1996. A structural investigation of CaO-Al_2O_3 glasses via ^{27}Al MAS-NMR. *Journal of Non-Crystalline Solids* **195**, 261-271.
McMillan, P.F., Piriou, B., 1983. Raman spectroscopy of calcium aluminate glasses and crystals. *Journal of Non-Crystalline Solids* **55**, 221-242.
McMillan, P.F., Wilding, M.C., 2008. Direct density determination of low- and high-density glassy polyamorphs following a liquid-liquid phase transition in Y_2O_3-Al_2O_3 supercooled liquids. *Journal of Non-Crystalline Solids* **354**, 1015-1025.
McMillan, P.F., Wilson, M., Wilding, M.C., 2003. Polyamorphism in aluminate liquids. *Journal of Physics:*

Condensed Matter **15**, 6105-6121.
McMillan, P.F., Wilson, M.,. Wilding, M.C.,. Daisenberger, D.,. Mezouar, M.,. Greaves, G.N., 2007. Polyamorphism and liquid-liquid phase transitions: challenges for experiment and theory. *Journal of Physics: Condensed Matter* **19**, 415101.
Mei, Q., Benmore, C.J., Siewenie, J., Weber, J.K.R., Wilding, M., 2008a. Diffraction study of calcium aluminate glasses and melts: I. High energy x-ray and neutron diffraction on glasses around the eutectic composition. *Journal of Physics: Condensed Matter* **20**, 245106. https://doi.org/10.1088/0953-8984/20/24/245106
Mei, Q., Benmore, C.J., Weber, J.K.R., Wilding, M., Kim, J., Rix, J., 2008b. Diffraction study of calcium aluminate glasses and melts: II. High energy x-ray diffraction on melts. *Journal of Physics: Condensed Matter* **20**, 245107. https://doi.org/10.1088/0953-8984/20/24/245107
Merzbacher, C.I., White, W.B., 1991. The structure of alkaline earth aluminosilicate glasses as determined by vibrational spectroscopy. *Journal of Non-Crystalline Solids* **130**, 18-34.
Moesgaard, M., Keding, R., Skibsted, J., Yue, Y., 2010. Evidence of Intermediate-Range Order Heterogeneity in Calcium Aluminosilicate Glasses. *Chemistry of Materials* **22**, 4471-4483. https://doi.org/10.1021/cm1011795
Mongalo, L., Lopis, A.S., Venter, G.A., 2016. Molecular dynamics simulations of the structural properties and electrical conductivities of CaO-MgO-Al_2O_3-SiO_2 melts. *Journal of Non-Crystalline Solids* **452**, 194-202. https://doi.org/10.1016/j.jnoncrysol.2016.08.042
Morikawa, H., Marumo, F., Koyama, T., Yamane, M., Oyobe, A., 1983. Structural analysis of $12CaO.7Al_2O_3$ glass. *Journal of Non-Crystalline Solids* **56**, 355-360. https://doi.org/10.1016/0022-3093(83)90493-3
Morikawa, H., Miwa, S.-I., Miyake, M., Marumo, F., Sata, T., 1982. Structural Analysis of SiO_2-Al_2O_3 Glasses. *Journal of the American Ceramic Society* **65**, 78-81. https://doi.org/10.1111/j.1151-2916.1982.tb10361.x
Moulton, B.J.A., Henderson, G.S., Sonneville, C., O'Shaughnessy, C., Zuin, L., Regier, T., de Ligny, D., 2016. The structure of haplobasaltic glasses investigated using X-ray absorption near edge structure (XANES) spectroscopy at the Si, Al, Mg, and O K -edges and Ca, Si, and Al L2,3 -edges. *Chemical Geology* **420**, 213-230. https://doi.org/10.1016/j.chemgeo.2015.11.016
Murdoch, J.B., Stebbins, J.F.,. Carmichael, I.S.E., 1985. High-resolution ^{29}Si NMR study of silicate and aluminosilicate glasses: the effect of network modifying cations. *American Mineralogist* **70**, 332-343.
Mysen, B.O., 1990. Role of Al in depolymerized, peralkaline aluminosiliscate melts in the systems Li_2O-Al_2O_3-SiO_2, Na_2O-Al_2O_3-SiO_2, K_2O-Al_2O_3-SiO_2. *American Mineralogist* **75**, 120-134.
Mysen, B.O., Toplis, M.J., 2007. Structural behavior of Al^{3+} in peralkaline, metaluminous, and peraluminous silicate melts and glasses at ambient pressure. *American Mineralogist* **92**, 933-946.
Nasikas, N.K., Sen, S., Papatheodorou, G.N., 2011. Structural Nature of Polyamorphism in Y_2O_3-Al_2O_3 Glasses. *Chemistry of Materials* **23**, 2860-2868. https://doi.org/10.1021/cm200241c
Navrotsky, A., Peraudeau, G.,. McMillan, P.F.,. Coutures, J.P., 1982. A thermochemical study of glasses and crystals along the joins silica-calcium aluminate and silica-sodium aluminate. *Geochimica et Cosmochimica Acta* **46**, 2039-2047.
Neuville, D.R., Cormier, L., Flank, A.-M., Briois, V., Massiot, D., 2004a. Al speciation and Ca environment in calcium aluminosilicate glasses and crystals by Al and Ca K-edge X-ray absorption spectroscopy. *Chemical Geology* **213**, 153-163.
Neuville, D.R., Cormier, L., Massiot, D., 2006. Al coordination and speciation in calcium aluminosilicate glasses: effects of composition determined by ^{27}Al MQ-MAS NMR and Raman spectroscopy. *Chemical Geology* **229**, 173-185.
Neuville, D.R., Cormier, L., Massiot, D., 2004b. Al environment in tectosilicate and peraluminous glasses: a ^{27}Al MQ-MAS NMR, Raman, and EXAFS investigation. *Geochimica et Cosmochimica Acta* **68**, 5071-5079.
Neuville, D.R., Cormier, L., Montouillout, V., Florian, P., Millot, F., Rifflet, J.-C., Massiot, D., 2008. Structure of Mg- and Mg/Ca aluminosilicate glasses: ^{27}Al NMR and Raman spectroscopy investigations. *American Mineralogist* **93**, 1721-1731.
Neuville, D.R., Cormier, L., Montouillout, V., Massiot, D., 2007. Local Al site distribution in aluminosilicate glasses by ^{27}Al MQMAS NMR. *Journal of Non-Crystalline Solids* **353**, 180-184. https://doi.org/10.1016/j.jnoncrysol.2006.09.035
Neuville, D.R., Henderson, G.H., Cormier, L., Massiot, D., 2010. The structure of crystals, glasses, and melts along the CaO-Al_2O_3 join: Results from Raman, Al L- and K-edge X-ray absorption, and ^{27}Al NMR spectroscopy. *American Mineralogist* **95**, 1580-1589.
Nie, S., Thomsen, R.M., Skibsted, J., 2020. Impact of Mg substitution on the structure and pozzolanic reactivity of calcium aluminosilicate (CaO-Al_2O_3-SiO_2) glasses. *Cement and Concrete Research* **138**, 106231. https://doi.org/10.1016/j.cemconres.2020.106231
Novikov, A., 2017. Structure and dynamics of aluminosilicate glasses and melts. PhD Thesis. Université d'Orléans, Orléans, France.

Novikov, A.N., Neuville, D.R., Hennet, L., Gueguen, Y., Thiaudière, D., Charpentier, T., Florian, P., 2017. Al and Sr environment in tectosilicate glasses and melts: Viscosity, Raman and NMR investigation. *Chemical Geology* **461**, 115-127. https://doi.org/10.1016/j.chemgeo.2016.11.023

Okhotnikov, K., Stevensson, B., Edén, M., 2013. New interatomic potential parameters for molecular dynamics simulations of rare-earth (RE = La, Y, Lu, Sc) aluminosilicate glass structures: exploration of RE^{3+} field-strength effects. *Physical Chemistry Chemical Physics* **15**, 15041. https://doi.org/10.1039/c3cp51726h

Okuno, M., Zotov, N.,. Schmücker, M.,. Schneider, H., 2005. Structure of Al_2O_3-SiO_2 glasses: combined X-ray diffraction, IR and Raman studies. *Journal of Non-Crystalline Solids* **351**, 1032-1038.

Onoda, G.Y., Brown, S.D., 1970. Low-Silica Glasses Based on Calcium Aluminates. *Journal of the American Ceramic Society* **53**, 311-316. https://doi.org/10.1111/j.1151-2916.1970.tb12114.x

Pahari, B., Iftekhar, S., Jaworski, A., Okhotnikov, K., Jansson, K., Stevensson, B., Grins, J., Edén, M., 2012. Composition-Property-Structure Correlations of Scandium Aluminosilicate Glasses Revealed by Multinuclear ^{45}Sc, ^{27}Al, and ^{29}Si Solid-State NMR. *Journal of the American Ceramic Society* **95**, 2545-2553. https://doi.org/10.1111/j.1551-2916.2012.05288.x

Park, S.Y., Lee, S.K., 2018. Probing the structure of Fe-free model basaltic glasses: A view from a solid-state ^{27}Al and ^{17}O NMR study of Na-Mg silicate glasses, Na_2O-MgO-Al_2O_3-SiO_2 glasses, and synthetic Fe-free KLB-1 basaltic glasses. *Geochimica et Cosmochimica Acta* **238**, 563-579. https://doi.org/10.1016/j.gca.2018.07.032

Park, S.Y., Lee, S.K., 2014. High-resolution solid-state NMR study of the effect of composition on network connectivity and structural disorder in multi-component glasses in the diopside and jadeite join: Implications for structure of andesitic melts. *Geochimica et Cosmochimica Acta* **147**, 26-42. https://doi.org/10.1016/j.gca.2014.10.019

Park, S.Y., Lee, S.K., 2012. Structure and disorder in basaltic glasses and melts: Insights from high-resolution solid-state NMR study of glasses in diopside-Ca-tschermakite join and diopside-anorthite eutectic composition. *Geochimica et Cosmochimica Acta* **80**, 125-142. https://doi.org/10.1016/j.gca.2011.12.002

Pechenik, A., Susman, S., Whitmore, D., Ratner, M., 1986. Ionic conductivity in glasses: A Monte-Carlo study of ordered and disordered one-dimensional models. *Solid State Ionics* **18-19**, 403-409. https://doi.org/10.1016/0167-2738(86)90150-5

Pechenik, A., Whitmore, D.H., Susman, S., Ratner, M.A., 1988. Transport in glassy fast-ion conductors. *Journal of Non-Crystalline Solids* **101**, 54-64. https://doi.org/10.1016/0022-3093(88)90368-7

Petkov, V., Billinge, S.J.L.,. Shastri, S.D.,. Himmel, B., 2000. Polyhedral units and network connectivity in calcium aluminosilicate glasses from high-energy X-ray diffraction. *Physical Review Letters* **85**, 3436-3439.

Pfleiderer, P., Horbach, J.,. Binder, K., 2006. Structure and transport properties of amorphous aluminium silicates: computer simulation studies. *Chemical Geology* **229**, 186-197.

Poe, B.T., McMillan, P.F., Angell, C.A., Sato, R.K., 1992. Al and Si coordination in SiO_2-Al_2O_3 glasses and liquids - A study by NMR and IR spectroscopy and MD simulations. *Chemical Geology* **96**, 333-349. https://doi.org/10.1016/0009-2541(92)90063-b

Poe, B.T., McMillan, P.F.,. Coté, B.,. Masiot, D.,. Coutres, J.P., 1994. Structure and dynamics in calcium aluminate liquids: high-temperature 27Al NMR and Raman spectroscopy. *Journal of the American Ceramic Society* **77**, 1832-1838.

Ponader, C.W., Brown, G.E., 1989. Rare earth elements in silicate systems: I. Effects of composition on the coordination environments of La, Gd, and Yb. *Geochimica et Cosmochimica Acta* **53**, 2893-2903. https://doi.org/10.1016/0016-7037(89)90166-X

Ren, J., Zhang, L., Eckert, H., 2014. Medium-Range Order in Sol-Gel Prepared Al_2O_3-SiO_2 Glasses: New Results from Solid-State NMR. *The Journal of Physical Chemistry C* **118**, 4906-4917. https://doi.org/10.1021/jp412774h

Richet, P., Roskosz, M., Roux, J., 2006. Glass formation in silicates: insights from composition. *Chemical Geology* **225**, 388-401.

Riebling, E.F., 1966. Structure of Sodium Aluminosilicate Melts Containing at Least 50 mole % SiO_2 at 1500°C. *Journal of Chemical Physics* **44**, 2857-2865. https://doi.org/10.1063/1.1727145

Risbud, S.H., 1982. STEM and EELS analysis of multiphase microstructures in oxide and non-oxide glasses. *Journal of Non-Crystalline Solids* **49,** 241-251. https://doi.org/10.1016/0022-3093(82)90122-3

Risbud, S.H., Kirkpatrick, R.J., Taglialavore, A.P., Montez, B., 1987. Solid-state NMR Evidence of 4-, 5, and 6-Fold Aluminum Sites in Roller-Quenched SiO_2-Al_2O_3 Glasses. *Journal of the American Ceramic Society* **70**, C-10-C-12. https://doi.org/10.1111/j.1151-2916.1987.tb04859.x

Risbud, S.H., Pask, J.A., 1977. Calculated Thermodynamic Data and Metastable Immiscibility in the System SiO_2-Al_2O_3. *Journal of the American Ceramic Society* **60**, 418-424. https://doi.org/10.1111/j.1151-2916.1977.tb15525.x

Rosales-Sosa, G.A., Masuno, A., Higo, Y., Inoue, H., 2016. Crack-resistant Al_2O_3-SiO_2 glasses. *Scientific*

Reports **6**, 23620. https://doi.org/10.1038/srep23620
Rosales-Sosa, G.A., Masuno, A., Higo, Y., Inoue, H., Yanaba, Y., Mizoguchi, T., Umada, T., Okamura, K., Kato, K., Watanabe, Y., 2015. High Elastic Moduli of a $54Al_2O_3$-$46Ta_2O_5$ Glass Fabricated via Containerless Processing. *Scientific Reports* **5**, 15233. https://doi.org/10.1038/srep15233
Rosales-Sosa, G.A., Masuno, A., Higo, Y., Watanabe, Y., Inoue, H., 2018. Effect of rare-earth ion size on elasticity and crack initiation in rare-earth aluminate glasses. *Journal of the American Ceramic Society* **101**, 5030-5036. https://doi.org/10.1111/jace.15760
Rosenflanz, A., Frey, M., Endres, B., Anderson, T., Richards, E., Schardt, C., 2004. Bulk glasses and ultrahard nanoceramics based on alumina and rare-earth oxides. *Nature* **430**, 761-764. https://doi.org/10.1038/nature02729
Ross, S., Welsch, A.-M., Behrens, H., 2015. Lithium conductivity in glasses of the Li_2O-Al_2O_3-SiO_2 system. *Physical Chemistry Chemical Physics* **17**, 465-474. https://doi.org/10.1039/C4CP03609C
Roy, B.R., Navrotsky, A., 1984. Thermochemistry of charge-coupled substitutions in silicate glasses: the systems M1/nn+AlO_2-SiO_2 (M=Li, Na, K, Rb, Cs, Mg, Ca, Sr, Ba, Pb. *Journal of the American Ceramic Society* **67**, 606-610.
Sato, R.K., McMillan, P.F., Dennison, P., Dupree, R., 1991. High-resolution ^{27}Al and ^{29}Si MAS NMR investigation of SiO_2-A_2O_3 glasses. *The Journal of Physical Chemistry B* **95**, 4483-4489.
Schaller, T., Stebbins, J.F., 1998. The Structural Role of Lanthanum and Yttrium in Aluminosilicate Glasses: A ^{27}Al and ^{17}O MAS NMR Study. *The Journal of Physical Chemistry B* **102**, 10690-10697. https://doi.org/10.1021/jp982387m
Schmücker, M., MacKenzie, K.J.D.,. Schneider, H.,. Meinhold, R., 1997. NMR studies on rapidly solidified SiO_2-$Al2_2O_3$ and SiO_2O_3-Al_2O_3-Na_2O_3O glasses. *Journal of Non-Crystalline Solids* **217**, 99-105.
Schmücker, M., Schneider, H., 2002. New evidence for tetrahedral triclusters in aluminosilicate glasses. *Journal of Non-Crystalline Solids* **311**, 211-215. https://doi.org/10.1016/S0022-3093(02)01632-0
Schmücker, M., Schneider, H., 1996. A new approach on the coordination of al in non-crystalline gels and glasses of the system Al_2O_3-SiO_2. *Berichte der Bunsengesellschaft für Physikalische Chemie* **100**, 1550-1553. https://doi.org/10.1002/bbpc.19961000940
Sen, S., 2000. Atomic environment of high-field strength Nd and Al cations as dopants and major components in silicate glasses: a Nd LIII-edge and Al K-edge X-ray absorption spectroscopic study. *Journal of Non-Crystalline Solids* **261**, 226-236.
Sen, S., Stebbins, J.F., 1995. Structural role of Nd^{3+} and Al^{3+} cations in SiO_2 glass: a ^{29}Si MAS-NMR spin-lattice relaxation, ^{27}Al NMR and EPR study. *Journal of Non-Crystalline Solids* **188**, 54-62. https://doi.org/10.1016/0022-3093(95)00099-2
Sen, S., Youngman, R.E., 2004. High-Resolution Multinuclear NMR Structural Study of Binary Aluminosilicate and Other Related Glasses. *The Journal of Physical Chemistry B* **108**, 7557-7564. https://doi.org/10.1021/jp031348u
Shannon, R.D., 1976. Revised effective ionic radii and systematic studies of interatomic distance in halides and chalcogenides. *Acta Crystallographica* **A32**, 751-767.
Shelby, J.E., 1994. Rare Earths as Major Components in Oxide Glasses. *Key Enggineering Materials* **94-95**, 1-42. https://doi.org/10.4028/www.scientific.net/KEM.94-95.1
Shelby, J.E., 1978. Viscosity and thermal expansion of lithium aluminosilicate glasses. *Journal of Applied Physics* **49**, 5885-5891.
Shelby, J.E., Kohli, J.T., 1990. Rare-earth aluminosilicate glasses. *Journal of the American Ceramic Society* **73**, 39-42.
Shelby, J.E., Shaw, C.M.,. Spess, M.S., 1989. Calcium fluoroaluminate glasses. *Journal of Applied Physics* **66**, 1149-1154.
Shelby, J.E., Wierzbicki, M.M., 1995. Formation and properties of soda lime aluminate glasses. *Physics and Chemistry of Glasses* **36**, 17-21.
Skibsted, J., Henderson, E., Jakobsen, H.J., 1993. Characterization of calcium aluminate phases in cements by aluminum-27 MAS NMR spectroscopy. *Inorganic Chemistry* **32**, 1013-1027. https://doi.org/10.1021/ic00058a043
Skinner, L.B., Barnes, A.C., Crichton, W., 2006. Novel behaviour and structure of new glasses of the type Ba-Al-O and Ba-Al-Ti-O produced by aerodynamic levitation and laser heating. *Journal of Physics: Condensed Matter* **18**, L407-L414. https://doi.org/10.1088/0953-8984/18/32/l01
Skinner, L.B., Barnes, A.C., Salmon, P.S., Crichton, W.A., 2008. Phase separation, crystallization and polyamorphism in the Y_2O_3-Al_2O_3 system. *Journal of Physics: Condensed Matter* **20**, 205103. https://doi.org/10.1088/0953-8984/20/20/205103
Skinner, L.B., Barnes, A.C., Salmon, P.S., Fischer, H.E., Drewitt, J.W.E., Honkimäki, V., 2012. Structure and triclustering in Ba-Al-O glass. *Physical Review B* **85**, 064201. https://doi.org/10.1103/PhysRevB.85.064201

Smedskjaer, M.M., Huang, L., Scannell, G., Mauro, J.C., 2012. Elastic interpretation of the glass transition in aluminosilicate liquids. *Physical Review B* **85**, 144203. https://doi.org/10.1103/PhysRevB.85.144203

Smedskjaer, M.M., Mauro, J.C., Kjeldsen, J., Yue, Y., 2013. Microscopic Origins of Compositional Trends in Aluminosilicate Glass Properties. *Journal of the American Ceramic Society* **96**, 1436-1443. https://doi.org/10.1111/jace.12298

Smedskjaer, M.M., Youngman, R.E., Mauro, J.C., 2014. Principles of Pyrex® glass chemistry: structure-property relationships. *Applied Physics A* **116**, 491-504. https://doi.org/10.1007/s00339-014-8396-1

Stamboulis, A., Hill, R.G., Law, R.V., 2004. Characterization of the structure of calcium alumino-silicate and calcium fluoro-alumino-silicate glasses by magic angle spinning nuclear magnetic resonance (MAS-NMR. *Journal of Non-Crystalline Solids* **333**, 101-107. https://doi.org/10.1016/j.jnoncrysol.2003.09.049

Stebbins, J.F., Dubinsky, E.V., Kanehashi, K., Kelsey, K.E., 2008. Temperature effects on non-bridging oxygen and aluminum coordination number in calcium aluminosilicate glasses and melts. *Geochimica et Cosmochimica Acta* **72**, 910-925. https://doi.org/10.1016/j.gca.2007.11.018

Stebbins, J.F., Farnan, I., 1992. Effects of High Temperature on Silicate Liquid Structure: A Multinuclear NMR Study. *Science* **255**, 586-589. https://doi.org/10.1126/science.255.5044.586

Stebbins, J.F., Kroeker, S.,. Lee, S.K.,. Kiczenski, T.J., 2000. Quantification of five- and six-coordinated aluminium ions in aluminosilicate and fluoride-containing glasses by high-field, high-resolution ^{27}Al NMR. *Journal of Non-Crystalline Solids* **275**, 1-6.

Stebbins, J.F., Lee, S.K.,. Oglesby, J.V., 1999. Al-O-Al oxygen sites in crystalline aluminates and aluminosilicates glasses: high resolution oxygen-17 NMR results. *American Mineralogist* **84**, 983-986.

Stebbins, J.F., Xu, Z., 1997. NMR evidence for excess non-bridging oxygen in an aluminosilicate glass. *Nature* **390**, 60-62. https://doi.org/10.1038/36312

Stein, D.J., Spera, F.J., 1995. Molecular dynamics simulations of liquids and glasses in the system $NaAlSiO_4$-SiO_2: methodology and melt structures. *American Mineralogist* **80**, 417-431.

Stevensson, B., Edén, M., 2013. Structural rationalization of the microhardness trends of rare-earth aluminosilicate glasses: Interplay between the RE^{3+} field-strength and the aluminum coordinations. *Journal of Non-Crystalline Solids* **378**, 163-167. https://doi.org/10.1016/j.jnoncrysol.2013.06.013

Sukenaga, S., Florian, P., Kanehashi, K., Shibata, H., Saito, N., Nakashima, K., Massiot, D., 2017. Oxygen Speciation in Multicomponent Silicate Glasses Using Through Bond Double Resonance NMR Spectroscopy. *Journal of Physical Chemistry Letters* **8**, 2274-2279. https://doi.org/10.1021/acs.jpclett.7b00465

Sun, K.-H., 1947. Fundamental conditions of glass formation. *Journal of the American Ceramic Society* **30**, 277-281. https://doi.org/10.1111/j.1151-2916.1947.tb19654.x

Sung, Y. -M., Kwon, S. -J., 1999. Glass-forming ability and stability of calcium aluminate optical glasses. *Journal of Materials Science Letters* **18**, 1267-1269. https://doi.org/10.1023/A:1006680506578

Takahashi, S., Neuville, D.R., Takebe, H., 2015. Thermal properties, density and structure of percalcic and peraluminus CaO-Al_2O_3-SiO_2 glasses. *Journal of Non-Crystalline Solids* **411**, 5-12. https://doi.org/10.1016/j.jnoncrysol.2014.12.019

Tanabe, S., Hirao, K., Soga, N., 1992. Elastic Properties and Molar Volume of Rare-Earth Aluminosilicate Glasses. *Journal of the American Ceramic Society* **75**, 503-506. https://doi.org/10.1111/j.1151-2916.1992.tb07833.x

Tandia, A., Timofeev, N.T., Mauro, J.C., Vargheese, K.D., 2011. Defect-mediated self-diffusion in calcium aluminosilicate glasses: A molecular modeling study. *Journal of Non-Crystalline Solids* **357**, 1780-1786. https://doi.org/10.1016/j.jnoncrysol.2010.12.078

Tangeman, J.A., Phillips, B.L.,. Nordine, P.C.,. Weber, J.K.R., 2004. Thermodynamics and structure of single- and two-phase yttria-alumina glasses. *The Journal of Physical Chemistry B* **108**, 10663-10671.

Thomas, B.W.M., Mead, R.N., Mountjoy, G., 2006. A molecular dynamics study of the atomic structure of $(CaO)x(Al_2O_3)1-x$glass with x= 0.625 close to the eutectic. *Journal of Physics: Condensed Matter* **18**, 4697-4708. https://doi.org/10.1088/0953-8984/18/19/021

Thompson, L.M., Stebbins, J.F., 2013. Interaction between composition and temperature effects on non-bridging oxygen and high-coordinated aluminum in calcium aluminosilicate glasses. *American Mineralogist* **98**, 1980-1987. https://doi.org/10.2138/am.2013.4511

Thompson, L.M., Stebbins, J.F., 2012. Non-stoichiometric non-bridging oxygens and five-coordinated aluminum in alkaline earth aluminosilicate glasses: Effect of modifier cation size. *Journal of Non-Crystalline Solids* **358**, 1783-1789. https://doi.org/10.1016/j.jnoncrysol.2012.05.022

Thompson, L.M., Stebbins, J.F., 2011. Non-bridging oxygen and high-coordinated aluminum in metaluminous and peraluminous calcium and potassium aluminosilicate glasses: High-resolution ^{17}O and ^{27}Al MAS NMR results. *American Mineralogist* **96**, 841-853.

Toplis, M., Dingwell, D.B., 2004. Shear viscosities of CaO-Al_2O_3-SiO_2 and MgO-Al_2O_3-SiO_2 liquids: Implications for the structural role of aluminium and the degree of polymerisation of synthetic and natural

aluminosilicate melts. *Geochimica et Cosmochimica Acta* **68**, 5169-5188.
Toplis, M.J., Dingwell, D.B., Hess, K.-U., Lenci, T., 1997a. Viscosity, fragility, and configurational entropy of melts along the join SiO_2-$NaAlSiO_4$. *American Mineralogist* **82**, 979-990.
Toplis, M.J., Dingwell, D.B., Lenci, T., 1997b. Peraluminous viscosity maxima in Na_2O-Al_2O_3-SiO_2 liquids: the role of triclusters in tectosilicate melts. *Geochimica et Cosmochimica Acta* **61**, 2605-2612.
Toplis, M.J., Kohn, S.C., Smith, M.E., Poplett, I.J.F., 2000. Fivefold-coordinated aluminium in tectosilicate glasses observed by triple quantum MAS NMR. *American Mineralogist* **85**, 1556-1560.
Tossell, J.A., Horbach, J., 2005. O Triclusters Revisited: Classical MD and Quantum Cluster Results for Glasses of Composition $(Al_2O_3)_2(SiO_2$. *The Journal of Physical Chemistry B* **109**, 1794-1797. https://doi.org/10.1021/jp0454873
Uhlmann, E.V., Weinberg, M.C.,. Kreidl, N.J.,. Goktas, A.A., 1993. Glass-forming ability in calcium aluminate-based systems. *Journal of the American Ceramic Society* **76**, 449-453.
Varshneya, A.K., Mauro, J.C., 2019. Fundamentals of inorganic glasses. 3rd Edition. Elsevier.
Veit, U., Rüssel, C., 2016. Density and Young′s Modulus of ternary glasses close to the eutectic composition in the CaO-Al_2O_3-SiO_2-system. *Ceramics International* **42**, 5810-5822. https://doi.org/10.1016/j.ceramint.2015.12.123
Wallenberger, F.T., Brown, S.D., 1994. High-modulus glass fibers for new transportation and infrastructure composites and new infrared uses. *Composites Science and Technology* **51**, 243-263. https://doi.org/10.1016/0266-3538(94)90194-5
Wang, J., Brocklesby, W.S., Lincoln, J.R., Townsend, J.E., Payne, D.N., 1993. Local structures of rare-earth ions in glasses: the 'crystal-chemistry' approach. *Journal of Non-Crystalline Solids* **163**, 261-267. https://doi.org/10.1016/0022-3093(93)91303-K
Wang, S., Stebbins, J.F., 2004. Multiple-Quantum Magic-Angle Spinning ^{17}O NMR Studies of Borate, Borosilicate, and Boroaluminate Glasses. *Journal of the American Ceramic Society* **82**, 1519-1528. https://doi.org/10.1111/j.1151-2916.1999.tb01950.x
Watanabe, Y., Masuno, A., Inoue, H., 2012. Glass formation of rare earth aluminates by containerless processing. *Journal of Non-Crystalline Solids* **358**, 3563-3566. https://doi.org/10.1016/j.jnoncrysol.2012.02.001
Watanabe, Y., Masuno, A., Inoue, H., Yanaba, Y., Kato, K., 2020. Influence of modifier cations on the local environment of aluminum in La_2O_3-Al_2O_3 and Y_2O_3-Al_2O_3 binary glasses. *Physical Chemistry Chemical Physics* **22**, 19592-19599. https://doi.org/10.1039/D0CP02778B
Weber, J.K.R., Felten, J.J., Cho, B., Nordine, P.C., 1998. Glass fibres of pure and erbium- or neodymium-doped yttria-alumina compositions. *Nature* **393**, 769-771. https://doi.org/10.1038/31662
Weber, J.K.R., Tangeman, J.A., Key, T.S., Hiera, K.J., Paradis, P.-F., Ishikawa, T., Yu, J., Yoda, S., 2002. Novel Synthesis of Calcium Oxide-Aluminum Oxide Glasses. *Japanese Journal of Applied Physics* **41**, 3029-3030. https://doi.org/10.1143/jjap.41.3029
Weber, R., Benmore, C.J., Siewenie, J., Urquidi, J., Key, T.S., 2004. Structure and bonding in single- and two-phase alumina-based glasses. *Physical Chemistry Chemical Physics* **6**, 2480-2483. https://doi.org/10.1039/B314957A
Weber, R., Sen, S., Youngman, R.E., Hart, R.T., Benmore, C.J., 2008. Structure of High Alumina Content Al_2O_3-SiO_2 Composition Glasses. *The Journal of Physical Chemistry B* **112**, 16726-16733. https://doi.org/10.1021/jp807964u
Wilding, M.C., Benmore, C.J.,. McMillan, P.F., 2002. A neutron difraction study of yttrium- and lanthanum-aluminate glasses. *Journal of Non-Crystalline Solids* **297**, 143-155.
Wilding, M.C., Benmore, C.J., Weber, J.K.R., 2010. High-Energy X-ray Diffraction from Aluminosilicate Liquids. *The Journal of Physical Chemistry B* **114**, 5742-5746. https://doi.org/10.1021/jp907587e
Wilding, M.C., McMillan, P.F., 2002. Liquid polymorphism in yttrium-aluminate liquids, in: New Kinds of Phase Transitions: Transformation in Disordered Substances, NATO Science Series. V. V. Brazhkin, S. V. Buldyrev, V. N. Rhzhov and H. E. Stanley, Dordrecht, Boston, pp. 57-73.
Wilding, M.C., McMillan, P.F., 2001. Polyamorphic transitions in yttria-alumina liquids. *Journal of Non-Crystalline Solids* **293-295**, 357-365.
Wilding, M.C., McMillan, P.F., Navrotsky, A., 2002. Thermodynamic and structural aspects of the polyamorphic transition in yttrium and other rare-earth aluminate liquids. *Physica A: Statistical Mechanics and its Applications* **314**, 379-390. https://doi.org/10.1016/S0378-4371(02)01045-2
Wiles, N.T., Goyal, S., Baker, S.P., 2020. Geometric configuration of five-coordinated Al and Si in tectosilicate calcium aluminosilicate glasses and its effect on plastic flow. *Journal of Non-Crystalline Solids* **543**, 120129. https://doi.org/10.1016/j.jnoncrysol.2020.120129
Winkler, A., Horbach, J., Kob, W., Binder, K., 2004. Structure and diffusion in amorphous aluminum silicate: A molecular dynamics computer simulation. *Journal of Chemical Physics* **120,** 384-393. https://doi.org/10.1063/1.1630562

Wu, J., Stebbins, J.F., 2009. Effects of cation field strength on the structure of aluminoborosilicate glasses: High-resolution ^{11}B, ^{27}Al and ^{23}Na MAS NMR. *Journal of Non-Crystalline Solids* **355**, 556-562. https://doi.org/10.1016/j.jnoncrysol.2009.01.025

Wu, Z., Romano, C.,. Marcelli, A.,. Mottana, A.,. Cibin, G.,. Della Ventura, G.,. Giuli, G., 1999. Evidence for Al/Si tetrahedral network in aluminosilicate glasses from Al K-edge x-ray-absorption spectroscopy. *Physical Review B* **60**, 9216-9219.

Xiang, Y., Du, J., Smedskjaer, M.M., Mauro, J.C., 2013. Structure and properties of sodium aluminosilicate glasses from molecular dynamics simulations. *Journal of Chemical Physics* **139**, 044507. https://doi.org/10.1063/1.4816378

Xue, X., Kanzaki, M., 2008. Structure of hydrous aluminosilicate glasses along the diopside-anorthite join: A comprehensive one- and two-dimensional ^{1}H and ^{27}Al NMR study. *Geochimica et Cosmochimica Acta* **72**, 2331-2348. https://doi.org/10.1016/j.gca.2008.01.022

Yamashita, H., Inoue, K., Nakajin, T., Inoue, H., Maekawa, T., 2003. Nuclear magnetic resonance studies of $0.139MO$ (or M'_2O)$\cdot 0.673SiO_2\cdot(0.188-x)Al_2O_3\cdot xB_2O_3$ (M=Mg, Ca, Sr and Ba, M′=Na and K) glasses. *Journal of Non-Crystalline Solids* **331**, 128-136. https://doi.org/10.1016/j.jnoncrysol.2003.08.086

Yarger, J.L., Smith, K.H.,. Nieman, R.A.,. Diefenbacher, J.,. Wolf, G.H.,. Poe, B.T.,. McMillan, P.F., 1995. Al coordination changes in high-pressure aluminosilicate liquids. *Science* **270**, 1964-1967.

Yeganeh-Haeri, A., Ho, C.T., Weber, R., Diefenbacher, J., McMillan, P.F., 1998. Elastic properties of aluminate glasses via Brillouin spectroscopy. *Journal of Non-Crystalline Solids* **241**, 200-203. https://doi.org/10.1016/S0022-3093(98)00804-7

Zachariasen, W.H., 1932. The atomic arrangement in glass. *Journal of the American Ceramic Society* **54**, 3841-3851.

Zhang, Y., Navrotsky, A., 2004. Thermochemistry of rare-earth aluminate and aluminosilicate glasses. *Journal of Non-Crystalline Solids* **341**, 141-151. https://doi.org/10.1016/j.jnoncrysol.2004.04.027

Zhang, Y., Navrotsky, A., 2003. Thermochemistry of Glasses in the Y_2O_3-Al_2O_3-SiO_2 System. *Journal of the American Ceramic Society* **86**, 1727-1732. https://doi.org/10.1111/j.1151-2916.2003.tb03547.x

Zheng, K., Zhang, Z., Yang, F., Sridhar, S., 2012. Molecular Dynamics Study of the Structural Properties of Calcium Aluminosilicate Slags with Varying Al_2O_3/SiO_2 Ratios. *ISIJ International* **52**, 342-349. https://doi.org/10.2355/isijinternational.52.342

Zirl, D.M., Garofalini, S.H., 1990. Structure of sodium aluminosilicate glasses. *Journal of the American Ceramic Society* **73**, 2848-2856.